# *A unified framework for trend uncertainty assessment in climate data records: demonstration on global mean sea level*

Surveys in Geophysics
https://doi.org/10.1007/s10712-025-09922-7

# A Unified Framework for Trend Uncertainty Assessment in Climate Data Records: Demonstration on Global Mean Sea Level

**Kevin Gobron[1,2] · Roland Hohensinn[3,4] · Xavier Loizeau[5] · Claire E. Bulgin[6,7] · Christopher J. Merchant[6,7] · Emma R. Woolliams[5] · Maurice G. Cox[5] · Wouter Dorigo[8] · Thomas Howard[5,9] · Mary Langsdale[10] · Adam C. Povey[11] · Michaël Ablain[12] · Janusz Bogusz[13] · Alexander Gruber[8] · Anna Klos[13] · Jonathan Mittaz[6]**

Received: 12 May 2025 / Accepted: 18 December 2025


**Abstract**
Trends of essential climate variables are often estimated from climate data records to quantify changes in the Earth system. An understanding of the uncertainty in a trend is essential for accurately determining the significance of a trend and attributing its causes. Despite this importance, trend-uncertainty estimates rarely account for all known sources of uncertainty. Common approaches neglect measurement-system instability or neglect the impact of natural variability on trend uncertainty. Such neglect can result in over-confidence in trend estimates. This study addresses trend-uncertainty assessment, particularly the need to account for the combined effects of measurement instability and natural variability on the trend uncertainty. The study presents a novel, unified framework for trend estimation that combines available measurement uncertainty information with empirical modelling of natural climate variability to achieve a more accurate uncertainty estimate. The framework is demonstrated for a time series of global mean sea level observations, obtaining more realistic trend-uncertainty values. The framework is applicable to most other climate data records. Adopting this approach will enhance confidence in climate change analysis through more accurate trend-uncertainty assessment in climate studies.

**Keywords** Trend estimation · Uncertainty · Climate data records · Essential climate variables · Natural variability · Measurement errors

## Article Highlights

- Approaches to assessing the uncertainty of trends estimated from climate data records overlook some uncertainty sources
- This study proposes a more complete trend uncertainty assessment by unifying current approaches
- The proposed approach is employed to quantify the uncertainty in the global mean sea level trend accurately

Extended author information available on the last page of the article

## 1 Introduction

Analysing trends in geophysical time series is a fundamental means of quantifying changes in the Earth system (Yang et al. 2013). Trends reflect geophysical processes arising both naturally and from anthropogenic forcing. The estimation of trends is critical to understanding and monitoring the impacts of human activity on the Earth system, and to assessing the resulting hazards for our societies (e.g., Intergovernmental Panel on Climate Change 2021; Thompson et al. 2015). Trends in essential climate variables (ECVs) evaluated from climate data records (CDRs) are used when testing climate models, such as those contributing to the Coupled Model Intercomparison Project (CMIP) (Eyring et al. 2016; Meehl et al. 2007), and in quantifying Earth's energy budget and water cycles (Meyssignac et al. 2023; Rodell et al. 2018; Dorigo et al. 2021). Trend analysis supports many societal services, from agriculture and food security to public health and disaster preparedness, and informs adaptation and mitigation strategies (Lobell et al. 2011; Watts et al. 2018; Rosenzweig et al. 2011).

Given their importance, trend estimates should be provided alongside realistic values of their uncertainty at a desired confidence level to ensure robust interpretation and decision-making. Without proper uncertainty quantification, the statistical significance and importance of trends may be misinterpreted, which risks undermining their credibility for both science and policy. The challenge for trend analysis is to separate long-term changes from natural climate variability and observational effects. Natural climate variability, arising from the chaotic component of climate dynamics, can obscure long-term trends and complicate their estimation, particularly at regional scales (Hawkins and Sutton 2009; Deser et al. 2012a; Maher et al. 2020; Yip et al. 2011). Observational limitations may include noise (i.e., random independent errors) and structured errors, such as step changes in measurement bias, long-term calibration drift or aliasing effects due to inconsistent temporal sampling (Merchant et al. 2017; Mudelsee 2014). The impact of these factors on trend estimation should be reflected in the associated trend-uncertainty estimate. Yet, there is no widely implemented approach for properly assessing the effect of both natural climate variability and observational limitations on trend estimates.

Trends can be determined using various trend estimators: parametric or non-parametric, linear or nonlinear (Mudelsee 2019). Irrespective of the estimator, two general approaches to trend uncertainty assessment have been employed for Earth science applications, namely, a measurement uncertainty-oriented approach and, more commonly, a time-series analysis-oriented approach. These approaches mainly differ in their assumptions about sources of uncertainty. Measurement uncertainty-oriented approaches seek to quantify the dominant effects (sources of error) that arise within and propagate through the data-processing chain, and which affect the values in the CDR (Merchant et al. 2017; Ablain et al. 2019; Mittaz et al. 2019). The measurement uncertainty (or error covariance) information thus obtained may be propagated through any trend estimator to evaluate the trend uncertainty arising from measurement uncertainty. Alternatively, time-series analysis-oriented approaches attempt to characterize the uncertainty solely from the empirical modelling of the post-fit residuals, that is, from the discrepancies between the fitted statistical model and the time series (Mudelsee 2014; Franzke 2012; Hughes and Williams 2010; Harris et al. 2019). In trend-analysis software, the time-series analysis-oriented approach is often built in.

Either of these approaches may (and, in general, will) miss significant components of trend uncertainty. The measurement uncertainty-oriented approach does not account for the uncertainty in trends arising from natural climate variability because that variability

is a property of the quantity of interest and not of the measurement. On the other hand, by analysing post-fit residuals, the time-series analysis-oriented approach can account for the combined influence of natural climate variability and some structures of measurement error, but does not account for trend uncertainty arising from any structure of measurement error (such as calibration drift) that can be absorbed by the statistical model.

Here, we propose a unified framework for trend-uncertainty assessment that combines the measurement-uncertainty-oriented and time-series-analysis-oriented approaches. Using this framework, components of trend uncertainty are not omitted, and more realistic trend uncertainty estimates are obtained. The framework is demonstrated for the analysis of a global mean sea level (GMSL) time series. Nonetheless, the framework is applicable to many other ECVs, and could improve the statistical interpretation of climate-trend signals. The need for a unified approach within uncertainty estimation is well established in other contexts (see annex A.3 ISO 2017), and this paper presents the specific theory and sound practice for climate-trend analysis.

The article proceeds as follows. Section 2 defines terminology associated with uncertainty assessment and then describes methods widely adopted for the trend-analysis of ECVs from CDRs (particularly CDRs obtained by Earth observation). The section concludes by discussing the limitations of these methods regarding trend-uncertainty assessment. To address these limitations, Sect. 3 presents a unified framework for analysing CDRs, applicable to parametric trend estimators. This framework addresses the deficiencies of widespread practices while being more complete yet practical for trend-uncertainty assessment. To demonstrate the new framework, Sect. 4 employs it for trend analysis of GMSL. Finally, conclusions are drawn in Sect. 5.

## 2 Trend Analysis for ECVs: Current Practices and Limitations

### 2.1 Terminology: Measurand, Trend, Stability, and Uncertainty

An important concept associated with the notion of uncertainty is the notion of ‘measurand’. According to the (current) third edition of the International Vocabulary of Metrology (VIM) for error and standard uncertainty (BIPM et al. 2012), the measurand denotes the quantity intended to be measured. When analysing CDRs, the measurand would be the (essential) climate variable of interest and would correspond to a vector of measurand values. In this context, trend analysis aims to provide a statistical descriptor of the measurand’s temporal evolution. In trend analysis, one could also consider the measurand to be the true ECV trend. The measurement process would thus include both the CDR production and the trend estimation steps. While this definition is possible, it is not used here because the notions of trend and trend uncertainty are not standardised in the literature.

The simplest form of trend is a constant change of the measurand value with time (Mudelsee 2019), quantified by a slope (‘the trend’) in the measured-value unit per time unit (usually per year or per decade). More generally, a trend may be nonlinear, for which a more complex mathematical representation may be appropriate. The term ‘linear trend’ refers to the slope of a first-order representation of change over a period of interest. The second-order (quadratic) change with time over a period of interest, known as the ‘acceleration’, is also a metric of great interest in climate studies. Most generally, ‘the trend’ might refer to any long-term (e.g., decadal or longer) systematic change of the

measurand. A trend in any of these senses may be partly obscured by variations occurring on shorter time scales (Franzke 2012). These variations can result from natural climate variability (e.g., Deser et al. 2012b), measurement errors (Merchant et al. 2017) or changes in the sampling regime (e.g., Hegerl and Zwiers 2011; Trenberth and Fasullo 2012) (or any combination).

While the term 'stability' is defined by the Global Climate Observing System (GCOS) to be 'the change in bias over time' of an observational system, Merchant et al. (2026) identify limitations of this definition and propose alternatives formally aligned with metrological conventions. Informally, '(standard) stability uncertainty' is the dispersion in trend values that arises from errors in the observational system, expressed as a standard deviation. The observational system includes the measurement instruments, their sampling characteristics, and all processing steps used to create the CDR. This definition is the analogue of the definitions in the VIM (BIPM et al. 2012). There, 'error' describes the (usually) unknown and unknowable difference between the measured value and a true or reference value, and 'uncertainty' describes the 'dispersion of values reasonably attributable to a measurand given a measured value'. Fuller descriptions of errors, uncertainties, and the importance of error correlation structures for Earth observations are given in, e.g., Mittaz et al. (2019); Woolliams et al. (2025).

Finally, we build on the above definitions of trend and stability to define the '(standard) trend uncertainty' as the dispersion in possible values that could be reasonably assigned to the estimated first-order representation of a CDR. With this definition, the trend uncertainty depends on both the stability uncertainty and an uncertainty representing how this first-order representation is limited by nonlinear (higher-order) variation, for example, from the ECV naturally varying in a chaotic manner.

### 2.2 Approaches to Trend Estimation

Various trend analyses are performed in current practice. The aim may be merely to detect the presence and sign of a trend in a time series. This is typically done with the Mann-Kendall statistics (Mann 1945; Kendall 1955) and its derivatives (Hirsch et al. 1982; Hirsch and Slack 1984; Hamed and Rao 1998). Others aim to extract the low-frequency component of the time series' to isolate and analyse long-term effects using smoothing methods (e.g., Ghil and Vautard 1991; Huang et al. 1998; Folland et al. 2001; Ghil et al. 2002; Mann 2004, 2008; Arguez et al. 2008). In this study, we focus on approaches to quantify the linear trend, as well as the trend and acceleration of underlying changes, over a period of interest, in the face of shorter-term natural variability.

To quantify an average trend over a period of interest, available methods may be divided into parametric and non-parametric methods (Mudelsee 2019). Parametric approaches fit a chosen multivariate functional model (that is, a mathematical model made of a sum of basic mathematical functions) to the time series of interest. The parameters of these models are estimated using optimization methods. The choice of optimization method is influenced by the prior information available (e.g., bounds on some parameter), the limitations of the data to be analysed (e.g., the presence of uncharacterised biases), and desired properties of the estimator (e.g., robust to outliers, unbiased, or minimum-variance). The simplest and most commonly used approach is Ordinary Least-Squares estimation (OLS). Other methods include Weighted and Generalised Least-Squares (WLS and GLS) estimation, Maximum Likelihood (ML) estimation, L1 norm minimization, and Maximum A Posteriori (MAP) estimation.

Besides such parametric methods, non-parametric trend estimation methods exist. These provide trend values from time series without specifying a functional model. The Theil-Sen trend estimator is an example of such a non-parametric estimator (Theil 1950; Sen 1968). This estimator provides a trend estimate by computing the median of all the pairwise slopes calculated between all the points of a time-series. It is often used when calculating trends in geophysical variables due to its robust performance in the presence of outliers (Fernandes and LeBlanc 2005).

### 2.3 Approaches to Trend Uncertainty Assessment

Although there is a wide variety of approaches to trend analysis, and trend estimation in particular, most approaches to trend uncertainty assessment involve propagating sources of uncertainty through the trend estimator used. The differences between uncertainty assessment approaches lie in the definition of these sources of uncertainty. We highlight two main practices: a measurement uncertainty-oriented approach and a time-series analysis-oriented approach.

#### 2.3.1 The Measurement Uncertainty-Oriented Approach

The measurement uncertainty-oriented approach is guided by metrological principles. These principles enable the construction of an uncertainty budget that considers known sources of uncertainty in the measurement process (BIPM et al. 2008; Mittaz et al. 2019; Woolliams et al. 2025). Assuming that all relevant effects can be identified and described, their associated uncertainties can, at least in principle, be propagated to the time series of the measurand that is to be the input to trend analysis. Because time-series analysis is often applied to highly aggregated derivatives of CDRs, such as large-scale monthly averages, accounting appropriately for the structured errors that are present in the full-resolution CDR is essential in this process. The result is the joint probability density function (or its representation as a covariance matrix) of the errors in the time series. This result can, in turn, be propagated, analytically or numerically, through the chosen trend estimator to obtain the trend uncertainty arising from measurement uncertainty. This approach is, for instance, (partially) employed by Ablain et al. (2019) to analyse the trend in GMSL.

#### 2.3.2 The Time-Series Analysis-Oriented Approach

CDRs do not always possess a measurement-uncertainty assessment adequate to define the error covariance matrix of a time series, even where good uncertainty practice (Merchant et al. 2017) is followed. Uncertainty in climate trends is thus commonly estimated using methods based on post-fit residuals. It is common naively to assume those residuals are independent and identically distributed (white noise), which is often a default in software implementations. More rigorously, the geoscience community approach to time-series analysis uses 'stochastic processes' to mimic the temporal structure of the post-fit residuals (Williams 2003). These stochastic processes may include white noise, power-law and auto-regressive processes. The specific choice for the stochastic process(es) is often *empirical* because it is guided by the study of the sample autocorrelation of the post-fit residuals (or of its power spectrum, in the frequency domain). Each process may also depend on unknown stochastic parameters, which can estimated from the measured values using so-called variance component estimation methods (Harville 1977). The trend uncertainty

is then obtained by propagating the covariance matrix of the stochastic process(es) through the trend estimator used. In climate studies, this time-series analysis-oriented approach has been used, for instance, to assess the uncertainty in sea-level change trends from ground-based or space-born sensors (Hughes and Williams 2010; Bos et al. 2014).

### 2.4 Examples of Trend Analysis for a Selection of Essential Climate Variables

ECV trends can be derived by CDR producers and users, leading to a large variety of approaches to trend uncertainty assessment. CDR producers understand the retrieval algorithms and uncertainties in their data, sometimes conducting metrological assessments. In contrast, CDR users come from varied backgrounds and focus on using ECV time series to address specific questions. They often lack insight into error characteristics and would benefit from guidance on data-set selection and appropriate trend estimators. To highlight the differences in the quantification of trends and their uncertainties, we adopt the data producer perspective and present a non-exhaustive selection of trend analysis methodologies for six Essential Climate Variables (ECVs) spanning the expertise of the authors: Land Surface Temperature (LST), Sea Surface Temperature (SST), aerosol optical depth (AOD), soil moisture, sea level, and terrestrial water storage:

- *Land-surface temperature*: LST data records span ~ 25 years, with measurements made using infrared and microwave sensors. These observations are critical to understand how the surface of the Earth is warming with climate change. To analyse long-term trends in LST CCI, monthly products are used. Trends can be calculated both for the LST, and LST minus two metre air temperature anomalies, to assess how strongly coupled these variables are. Trends are calculated using a Theil-Sen estimate, robust to outliers. A full uncertainty budget is provided with the monthly LST products, but is yet to be utilised in the trend analysis (e.g., Ghent et al. 2019; Good et al. 2022).
- *Sea-surface temperature*: Thermal infrared and microwave sensors have monitored the change in temperature over oceans for the last 44 years. These observations are essential for analysing ocean warming and confronting climate models. SST data are usually provided as daily products, often aggregated to de-seasonalised monthly products for trend analysis. The SST trends are typically estimated using the OLS estimator, assuming a linear or, sometimes, quadratic change. The trend uncertainties are obtained using variance propagation of the full uncertainty budget provided with the SST products (e.g., Embury et al. 2024; Merchant et al. 2025).
- *Aerosol optical depth*: For 30 years, visible and near-infrared sensors have monitored changes in the amount of light that aerosols scatter or absorb in a column of the atmosphere. Analysing AOD is essential for monitoring changes in radiative forcing and for public health applications. AOD data are most commonly used as daily or monthly products, often aggregated as de-seasonalised monthly products during trend analysis. The long-term trend in the aerosol optical depth is usually estimated using the OLS estimator, assuming a linear trend. The trend uncertainties are obtained by propagating the uncertainty of the measured values or by comparing them with a reference dataset (e.g., Yoon et al. 2016).
- *Soil moisture*: Passive and active microwave sensors provide estimates of soil water content since 1978. Analysing the variations in soil moisture is crucial to understanding how climate change and land use affect the water, energy, and biogeochemical. Soil moisture data are provided as monthly, seasonal, or yearly means, computed from

(irregular) daily data. The trends in soil moisture are typically estimated using OLS or the Theil-Sen estimator. The significances of the trends are calculated using Mann-Kendall statistics (e.g., Dorigo et al. 2012; Hirschi et al. 2025).

- *Sea level*: Radar altimeters have measured changes in sea levels over the oceans for 30 years. These measurements inform us about the global and regional sea-level variations caused by climate change. Sea-level data are provided as 10-day estimates or monthly means, and sometimes de-seasonalised for trend analysis. The trend in sea level is computed using OLS or GLS, assuming a linear trend with possible acceleration. The trend uncertainty is calculated by propagating the available covariance matrix describing instrumental uncertainties (e.g., Ablain et al. 2019; Meyssignac et al. 2023).
- *Terrestrial water storage*: space gravity missions have allowed changes in the gravity field to be measured for 22 years, and thereby enabled us to infer terrestrial water storage variations. The variations of terrestrial water storage inform us about the impact of climate change and anthropogenic activities on the water cycle. Space gravity data are provided as monthly products. The trend in terrestrial water storage is computed using (weighted) least-squares or Theil-Sen estimators (e.g., Scanlon et al. 2016; Humphrey et al. 2016). Trend estimation primarily relies on individual solutions, with uncertainties quantified using empirical covariance modelling (e.g., Boergens et al. 2022).

The data producer's approaches to trend estimation for this selection of examples vary in terms of data structure, trend estimation, and uncertainty assessment. The sea level, for example, benefits from a full covariance matrix of instrumental uncertainties that can be used for trend estimation and variance propagation. On the other hand, SST, LST, AOD, and soil moisture generate per-datum uncertainties for all measured values, but their propagation into trend estimation is still limited (Li et al. 2009; Bulgin et al. 2025). For LST and soil moisture, a non-parametric trend estimator is also sometimes preferred to reduce sensitivity to outliers, which may complicate uncertainty assessment. Currently, the terrestrial water storage data does not include bottom-up uncertainties; instead, it estimates sources of uncertainty statistically before variance propagation. Each of these approach suffer from uncertainty assessment limitations, which are discussed in the following section.

### 2.5 Uncertainty Assessment Limitations

Current uncertainty assessment approaches are subject to several limitations that should be considered when interpreting trend estimates. This section first emphasizes the need to consider generally overlooked limitations, applicable to all estimation approaches, such as sub-optimal sampling (Sect. 2.5.1) and defaults in auxiliary data stability (Sect. 2.5.2). Then, in addition to these general limitations affecting all estimation methods, this section presents additional limitations that are more specific to the trend-uncertainty assessment approaches discussed above (Sect. 2.5.3).

#### 2.5.1 Sampling, Aliasing, and Missing Measured Values

For both uncertainty assessment approaches, the impact of sampling, aliasing and missing data should be carefully considered and accounted for, for example as part of the measurement error covariance matrix. In many climate data records, spatial sampling

varies with time. This variation may relate to temporal changes in a given instrument record, e.g., orbital drift (Bulgin et al. 2018), or to changes over a sensor series, e.g., increasing sensor number or coverage in more recent years (Good et al. 2020). Aliasing is also possible due to the sampling regime, which may provide insufficient data to sample fully diurnal, tidal, or seasonal cycles.

Errors due to sampling also arise from the natural variability within the observed geophysical system, unrelated to the geophysical signal of interest. An example would be temporal variability in cloud cover. Retrieval of surface properties that are only possible under clear-sky conditions would be affected by the distribution of cloud, such that any correlation between cloud presence and the quantity of interest can bias the observational sample, an often overlooked source of error. Sampling variation and aliasing are often neglected as sources of measurement uncertainty and are not commonly propagated during uncertainty assessment. Where possible, these effects should be modelled and accounted for, but there may be insufficient information to do this fully. Practical approaches to this are reviewed in Langsdale et al. (2025), within the scope of intercomparing different datasets.

Intuitively, a lack of measured values caused by sampling limitations would increase the uncertainty of the estimated parameters. Where relevant, this uncertainty increase may be evaluated with respect to an alternative, and often hypothetical, situation in which more measured values are available (e.g., by comparing with estimates obtained when imputing virtual measured values).

### 2.5.2 Auxiliary Information Stability

Instability in ECV time-series can also result from temporal changes in the auxiliary data employed in the ECV retrieval. Many geophysical retrievals rely on auxiliary information, e.g., reanalysis data characterising the atmosphere through which an observation is made, or other observational data sets, e.g., for emissivity, to describe the Earth's surface. Temporal changes in the methods used to generate these auxiliary data sets can introduce non-geophysical signals into the ECV trends. Examples include updates to modelling systems generating numerical weather prediction data or increased sampling frequency of observational data sets.

Retrieval products may also depend on pre- or post-processing steps that aim to improve data quality. One such example is the identification of cloud-affected observations, which are important when retrieving surface, cloud and aerosol properties. This 'cloud screening' is carried out as a pre-processing step, the success rate of which depends both on the behaviour of the algorithm used and the characteristics of the individual sensor.

Because of the relatively short duration of many satellite missions, climate data records are usually constructed using data from multiple satellite missions. The available observational wavelengths or other characteristics differ between missions. Efforts are made to harmonize results, but nonetheless some level of non-geophysical instability in the time series may be introduced (Bulgin et al. 2024).

### 2.5.3 Approach-Specific Limitations

As explained in Sect. 2.3, most trend uncertainties are obtained by propagating modelled uncertainty through the employed trend estimator. Consequently, any overlooked uncertainty source will cause trend uncertainties to be misestimated.

As well as the sampling and auxiliary information issues described in the previous subsections, there are often other sources of uncertainty of which we are unaware (Povey and Grainger 2015). The different approaches to trend uncertainty propagation (Sect. 2.3), are likely to neglect different types of uncertainty sources, though these could be accounted for in principle.

**2.5.3.1 Measurement Uncertainty-Oriented Approach Limitations** A measurement uncertainty-oriented approach requires each source of uncertainty to be assessed and quantified sufficiently in isolation from other sources of uncertainty. In many ECV analyses, it can be difficult, or even impossible, to quantify some individual sources of uncertainty. Such sources remain neglected in the uncertainty budget either as 'known unknowns' (unquantifiable) or as 'unknown unknowns' (not yet identified). Within the laboratory environment of metrology institutes, such effects are often identified through comparisons with independent observations and become apparent when the absolute differences are larger than their associated expanded uncertainties. Such approaches are sometimes possible in Earth observations, e.g., through comparisons between satellite and in-situ data, but are usually limited to a small subset of observations.

The measurement uncertainty-oriented approach usually addresses only the uncertainty in the trend from uncertainty in individual measured values and computational process used by a data producer to produce the CDR. In other words, this approach quantifies the stability uncertainty, which ideally would also consider stability in sampling and auxiliary information. In many climate studies, we are additionally concerned with the uncertainty associated with the functional approximation to the geophysical processes; that is, the trend uncertainty induced by the unpredictable/chaotic component of the measurand (reflecting, for instance, nonlinear natural-climate variability (Ghil and Vautard 1991; Agnew 1992)) is also important. This uncertainty component from natural variability is, often by definition, omitted in the measurement uncertainty-oriented approach. This omission is in contrast to the time-series analysis-oriented approach, which would automatically consider both natural and part of the instrument system design variations.

**2.5.3.2 Time-Series Analysis-Oriented Approach Limitations** A time-series analysis-oriented approach relies solely on a data-driven characterisation of residuals to the fit, with no distinction made with respect to their origins as measurement errors or unfitted (natural phenomenon) variability. Though such an approach has the advantage of accounting for the influence of natural chaotic variability to some degree, it cannot account for measurement errors with temporal structures similar to the fitted mathematical model. That is, uncorrected long-term drifts and biases in the instruments, or due to sampling or auxiliary information stability, would be absorbed by the estimated (fitted) parameters and would not appear in the post-fit residuals.

Additionally, this approach relies on being able to model the noise empirically. The resulting trend uncertainty depends on the realism of the noise model and correlation assumptions. For instance, in many geoscientific applications, the naive assumption is that errors are time-independent and normally distributed (normal white noise). That assumption is usually inconsistent with the observation as it neglects temporal dependencies frequently observed in CDRs (Agnew 1992; Hughes and Williams 2010), and any inappropriate choice for the noise model may translate into a trend-uncertainty assessment error.

## 3 Approach for a Unified Uncertainty Assessment

To address the approach-specific limitations discussed in Sect. 2.5.3, this section introduces an alternative approach that combines available information on measurement uncertainty with empirical stochastic modelling of natural climate variability and unknown-but-quantifiable effects. This section starts by providing an alternative definition of a CDR that highlights the separate contributions of measurement errors and the variability of the quantity of interest (Sect. 3.1). The practical mathematical modelling of these components is detailed in Sects. 3.2 and 3.3. Building upon these mathematical definitions, Sect. 3.4 then highlights why the uncertainty assessment approaches discussed in Sect. 2.3 cannot converge to a single uncertainty estimate. To overcome this issue, Sect. 3.5 describes how to define the expectation and variance of the measured values in an alternative way, and Sect. 3.6 presents how these alternative expectation and variance definitions can be used to derive estimated parameters with realistic uncertainties. Since, in practice, our prior knowledge of the variance of the measured values can be incomplete, Sect. 3.7 proposes a more practical and flexible method for assessing the complete variance, which allows for empirical modelling. Altogether, this section describes a practical and unified uncertainty assessment approach for trend analysis.

### 3.1 Alternative Time-Series Model

Trend analysis usually requires modelling a series of measured values provided by a measuring system, constituting climate data records arranged in time order. We consider a time-indexed set of $m$ measured values $\mathbf{y} = [y_1, \ldots, y_m]$. Being a climate data record, it is assumed that the series has been previously corrected for all known and quantifiable effects that affect the measured signal without being part of the trend of interest, such as tidal signals or known instrumental drifts. It is important to recognise that there is an uncertainty associated with any such correction, which can be taken into account during the analysis step. In this analysis, we assume an additive error model (e.g., Brockwell and Davis 2002; Mudelsee 2019), in the form of what GUM-6 (BIPM et al. 2020, clause 11) calls a 'statistical model'. The measured value, $\mathbf{y}$, from the observations themselves can be thought of as the sum of a vector $\mathbf{Y}$, which represents the values of the measurand, that is, the quantity intended to be measured, and a measurement error vector, denoted by $\mathbf{E}$, that represents the signal due to observational system errors (including sampling effects, instrument drift, instrument noise, etc.). The measured value can thus be written:

$$\mathbf{y} = \mathbf{Y} + \mathbf{E}. \tag{1}$$

We recognise that a statistical model of a climate data record cannot always separate variations in the measurand $\mathbf{Y}$ from the measurement errors $\mathbf{E}$ for the reasons discussed above. Instead, we consider that functional variations (colloquially referred to as 'deterministic'), denoted by $\boldsymbol{\mu}$, are separated from non-functional variations, denoted by $\boldsymbol{\epsilon}$ (colloquially referred to as 'stochastic'). Here, *functional* means the analyst explicitly or implicitly proposes a structural variation in the form of mathematical functions of time or any other known variable (e.g., temperature, pressure, or outputs of numerical models). Conversely, *non-functional* means a structural variation for which no mathematical functions or numerical models are proposed. Instead, its structure is described probabilistically, by making the assumption that the observed non-functional variations, attributable to either $\mathbf{Y}$ or $\mathbf{E}$,

are realisations of latent random vectors with possibly intricate variance-covariance structures. This variance-covariance structure could be known *a priori* (measurement-uncertainty oriented approach) or assigned as part of the analysis (time-series analysis-oriented approach). Depending on the nature of the measured phenomenon, this non-functional term typically accounts for stochastic and/or aperiodic variations of the measurand. The difference between these components is illustrated in Fig. 1. Note, that we do not know the values of the parameters that define the functional form *a priori*, because if we did, they would be corrected in the previous correction.

Because both $\mathbf{Y}$ and $\mathbf{E}$ can represent diverse temporal patterns resulting from the complexity of the observed phenomenon and measuring system, none of these terms perfectly fits in the functional or the non-functional category, such that they may both be decomposed as

$$\begin{aligned} \mathbf{Y} &= \boldsymbol{\mu}_Y + \boldsymbol{\epsilon}_Y, \\ \mathbf{E} &= \boldsymbol{\mu}_E + \boldsymbol{\epsilon}_E, \end{aligned} \tag{2}$$

where

- $\boldsymbol{\mu}_Y$ is the part of the measurand $\mathbf{Y}$ described in a functional manner. These known functional forms have unknown functional parameters that we aim to estimate from the measured values. The functions are proposed from knowledge that may include prior theory, data inspection, or other reasoning. The functions may include linear

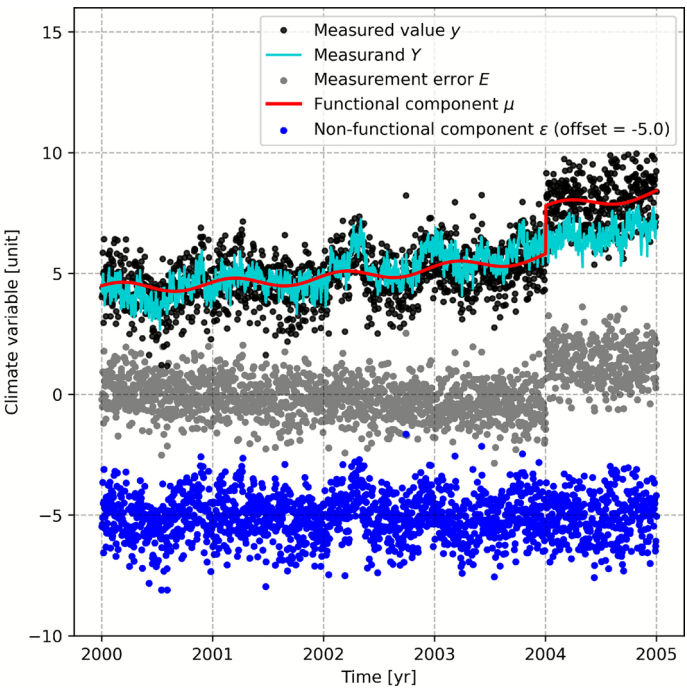


**Fig. 1** Synthetic illustration of the measured values $\mathbf{y}$, the measurand $\mathbf{Y}$, the measurement error $\mathbf{E}$, the functional component $\boldsymbol{\mu}$, and the non-functional component $\boldsymbol{\epsilon}$ (with an offset for legibility)

and higher-order trends, jumps, transients, periodic variations and time series of other phenomena expected to influence the measurand.

- $\boldsymbol{\epsilon}_Y$ is the non-functional part of the measurand, that is, the part that is not described functionally. This non-functional component can be described nonetheless using stochastic processes and their covariance matrices.
- $\boldsymbol{\mu}_E$ is the component of the measurement system (including sampling) error described functionally, often colloquially known as a systematic error in experimental conditions. As with the functional component of the measurand, this term can include, for instance, offsets, linear and non-linear drifts, periodic variations, and functions of other variables expected to influence the measurement error. The influence on measurement error may arise via the sensor performing the observations, or via auxiliary information used in the measurement model.
- $\boldsymbol{\epsilon}_E$ is the component of the measurement system error that varies with time in a non-functional manner, whether resulting from the measurement process or the corrections applied to the measured values. It includes random, independent measurement errors (although in a climate data record, these can be negligibly small in magnitude). It also includes structured errors for which no functional insight is available (or for which structural insight is available but not used to define a functional model for reasons of model parsimony). As for $\boldsymbol{\epsilon}_Y$, this non-functional component can be described using stochastic processes.

The above definitions of the functional components are subject to modelling decisions and are, to some degree, dependent on the expertise and preferences of the analyst. The key point is that, for completeness, all variations that are not functionally modelled *should* be accounted for in the stochastic modelling of the non-functional components. It is also important that functional and non-functional naming is chosen to emphasize that these are mathematical modelling choices, which are not necessarily correlated with the physical or instrumental effects that cause these variations. Understanding whether (non) functional components originate from systematic errors, random errors, natural variability, or anthropogenic forcing is a meaningful but separate concern.

According to this formulation, a measured value is considered an estimate $\mathbf{y}$ of the measurand $\mathbf{Y}$ that can be decomposed into four components such that

$$\mathbf{y} = \boldsymbol{\mu}_Y + \boldsymbol{\mu}_E + \boldsymbol{\epsilon}_Y + \boldsymbol{\epsilon}_E. \tag{3}$$

In first-order (linear) trend analysis, one element of the functional component vector $\boldsymbol{\mu}_Y$ is to be estimated, namely the coefficient of a monomial of degree one. The corresponding objective of trend-uncertainty assessment is to evaluate how all other components of the measured value equation affect the uncertainty in this trend coefficient. These other components include the remaining elements of $\boldsymbol{\mu}_Y$ (e.g., those modelling seasonal effects), the non-functional part of the measurand $\boldsymbol{\epsilon}_Y$, and the (non-)functional parts of the measurement errors ($\boldsymbol{\mu}_E$, $\boldsymbol{\epsilon}_E$). The following sections describe commonly occurring contributors to each component and how they may be mathematically modelled.

### 3.2 Functional-Component Models

Climate-data record time series often feature long-term trends, whether linear or nonlinear. Trends may reflect forced or unforced climatic change. Changes over time may also include more rapid discontinuities induced by geophysical events or the crossing of climate-tipping

points. Similar patterns of temporal change may also arise from measurement errors and sampling effects. Instrument calibration or other instrumental effects may introduce non-geophysical trends and discontinuities in climate data records. Such effects may reflect calibration drift within a single sensor (Dieng et al. 2017), whether from degradation or change in the sensor's operating environment from orbital drift (Christy et al. 2000; Mittaz et al. 2013). There may be relative biases between sensors, even within a harmonised record (Ablain et al. 2019; Zou et al. 2023). Natural or instrumental trends may be parametrically modelled with low-order polynomial functions of time (Bevis et al. 2020), whereas discontinuities may be modelled by modulating such polynomials using Heaviside functions.

As well as trends and discontinuities, climate data records often feature periodic variations reflecting, for instance, the ECV responses to Earth's rotation, orbit and tidal effects (Dong et al. 2002). Periodic variations can also result from measurement errors, e.g. caused by orbit-dependent effects on an instrument, non-modelled periodic influences on a retrieval, or miscorrection of undesired periodic effects (such as tide correction errors aliased through the sampling frequency). Periodic signals may be modelled using a linear combination of sinusoidal functions at appropriate reference frequencies and selected harmonics (since natural periodic signals are rarely purely sinusoidal) (Davis et al. 2012; Klos et al. 2018). These Fourier components may also be modulated with known functions, e.g., polynomials, to accommodate the fact that climate periodic signals are seldom constant in amplitude (de La Serve et al. 2023). Seasonal cycles are alternatively addressed by undertaking trend analysis on anomalies (departures from the climatological cycle over some defined period within the record).

Functional components can generally be represented as a linear(-ised) combination of known basis functions with possibly unknown amplitudes. In such a case, $\boldsymbol{\mu}_Y$ and $\boldsymbol{\mu}_E$ can be written as

$$\begin{aligned} \boldsymbol{\mu}_Y &= \mathbf{A}_Y \mathbf{x}_Y, \\ \boldsymbol{\mu}_E &= \mathbf{A}_E \mathbf{x}_E, \end{aligned} \tag{4}$$

where $\mathbf{A}_Y$ and $\mathbf{A}_E$ denote $m \times n_Y$ and $m \times n_E$ design matrices, whose columns correspond to known basis functions, while $\mathbf{x}_Y$ and $\mathbf{x}_E$ denote the $n_Y \times 1$ and $n_E \times 1$ unknown functional parameter vectors.

Equation 4 is linear, and written without a constant term since data analysis can always be done after subtracting constant values.

### 3.3 Non-functional-Component Modelling

In addition to functional variations, there is some variability that is not modelled functionally. Such variability can reflect the measurand's chaotic dynamics or its response to stochastic forcing (Ghil 2002). Measurement errors of various origins may have a structure that is hard to describe functionally. Noise is one example (whether independent or structured), and so are residual errors in corrections applied to the measured time series before analysis.

Non-functional variations are usually modelled using stochastic vectors, whose probability distributions (or just their covariance matrices under the normal distribution assumption) are determined from first principles or approximated using stochastic processes. These stochastic processes usually belong to the very general family of the Auto-Regressive Fractionally Integrated Moving Average processes (ARFIMA) (Granger

and Joyeux 1980; Hosking 1981), which encompass processes with short-memory (exponential-correlation decay) or long-memory effects (power-law correlation decay), observed in various types of geophysical and instrumental time-series (Press 1978; Agnew 1992; Hughes and Williams 2010).

In practice, these non-functional variations $\boldsymbol{\epsilon}_Y$ and $\boldsymbol{\epsilon}_E$ may be modelled in a stochastic manner by considering them as realisations of latent stochastic vectors, noted $\underline{\boldsymbol{\epsilon}}_Y$ and $\underline{\boldsymbol{\epsilon}}_E$ with zero-expectation. Under the normal distribution assumption, the random vector distributions are

$$\begin{aligned} \underline{\boldsymbol{\epsilon}}_Y &\sim \mathcal{N}(\mathbf{0}, \mathbf{Q}_Y), \\ \underline{\boldsymbol{\epsilon}}_E &\sim \mathcal{N}(\mathbf{0}, \mathbf{Q}_E), \end{aligned} \tag{5}$$

where $\mathbf{Q}_Y$ and $\mathbf{Q}_E$ denote $m \times m$ covariance matrices describing the dispersion and temporal structure of $\underline{\boldsymbol{\epsilon}}_Y$ and $\underline{\boldsymbol{\epsilon}}_E$.

Under the assumption of normal distribution, $\mathbf{Q}_Y$ and $\mathbf{Q}_E$ provide a complete description of $\underline{\boldsymbol{\epsilon}}_Y$ and $\underline{\boldsymbol{\epsilon}}_E$. These matrices may reflect a combination of effects with intricate time dependencies such that they are often non-diagonal. Although ideally, these matrices would be known, that would imply knowledge of the appropriate statistical distributions to describe the non-functional parts of the measurand (e.g., through the analysis of climate models or long time series of climate indices) and measurement error before interpreting the CDR (e.g., through complete metrological investigations of the measuring systems), which is still rare. In practice, parts of $\mathbf{Q}_Y$, $\mathbf{Q}_E$, or their sum, are partly empirically estimated from data, using stochastic modelling (Sect. 3.7).

### 3.4 Combination of Effects and Separability Issue

The above mathematical definitions clarify a fundamental issue of separability that makes it essential to use measurement uncertainty information when estimating trend uncertainties, whatever the method employed.

According to our measured-value model, Eq. (3), the measured vector is the sum of the values of the functional and non-functional components. The functional components of the measurand and the measurement errors, $\boldsymbol{\mu}_Y$ and $\boldsymbol{\mu}_E$, may include components represented by basis functions with common functional forms. For instance, the functional parts of the measurand and the measurement error can both contain a linear trend with unknown amplitudes, when assessing a trend with a climate data record that has an imperfectly known drift. In such cases, the matrices $\mathbf{A}_Y$ and $\mathbf{A}_E$ can be column partitioned (i.e., separating the columns relating to the common functional form) such that

$$\begin{aligned} \boldsymbol{\mu}_Y &= \bar{\mathbf{A}}\bar{\mathbf{x}}_Y + \breve{\mathbf{A}}_Y\breve{\mathbf{x}}_Y, \\ \boldsymbol{\mu}_E &= \bar{\mathbf{A}}\bar{\mathbf{x}}_E + \breve{\mathbf{A}}_E\breve{\mathbf{x}}_E, \end{aligned} \tag{6}$$

where $\bar{\mathbf{A}}$ is the $m \times n_C$ design matrix that relates to the common basis functions, $\bar{\mathbf{x}}_Y$ and $\bar{\mathbf{x}}_E$ are the corresponding unknown functional parameters, $\breve{\mathbf{A}}_Y$ and $\breve{\mathbf{A}}_E$ are the design matrices that relate to the component-specific basis functions, and $\breve{\mathbf{x}}_Y$ and $\breve{\mathbf{x}}_E$ are the corresponding unknown functional parameters.

According to the modelling assumptions made for each functional and non-functional component, the measured value model can be expanded as

$$\mathbf{y} = \bar{\mathbf{A}}(\bar{\mathbf{x}}_Y + \bar{\mathbf{x}}_E) + \breve{\mathbf{A}}_Y\breve{\mathbf{x}}_Y + \breve{\mathbf{A}}_E\breve{\mathbf{x}}_E + \boldsymbol{\epsilon}_Y + \boldsymbol{\epsilon}_E. \tag{7}$$

It is crucial to note that because the matrix $\bar{\mathbf{A}}$ relates to both $\bar{\mathbf{x}}_Y$ and $\bar{\mathbf{x}}_E$ in Eq. 7, $\bar{\mathbf{x}}_Y$ and $\bar{\mathbf{x}}_E$ cannot be estimated separately (only $\bar{\mathbf{x}}_Y + \bar{\mathbf{x}}_E$ can be estimated), unless external information is available to evaluate one or the other. This fundamental limitation is always present irrespective of the approach used for parameter or trend estimation, although it is not always recognised as being present.

In trend analysis, the trend-related elements in the vector of the geophysical parameters $\bar{\mathbf{x}}_Y$ constitute the component of interest and no direct estimate of $\bar{\mathbf{x}}_E$ is available. A metrological investigation could, however, lead to a probabilistic description of $\bar{\mathbf{x}}_E$. Such a description could be to assume that $\bar{\mathbf{x}}_E$ is a realisation of a zero-expectation random vector $\underline{\bar{\mathbf{x}}}_E$ such that $\underline{\bar{\mathbf{x}}}_E \sim \mathcal{N}(\mathbf{0}, \mathbf{Q}_{\bar{\mathbf{x}}_E})$. Here, it is assumed that $\underline{\bar{\mathbf{x}}}_E$ has zero expectation because any known functional error should be corrected before time-series analysis. As a result, $\underline{\bar{\mathbf{x}}}_E$ is a stochastic term, which will play a role when assessing the uncertainty associated with the estimated parameters.

### 3.5 Functional and Stochastic Models

With the stochastic modelling assumptions made above for $\boldsymbol{\epsilon}_Y$, $\boldsymbol{\epsilon}_E$, and $\bar{\mathbf{x}}_E$, the vector of measured values $\mathbf{y}$ can be considered as the realisation of a latent stochastic vector $\underline{\mathbf{y}}$ defined as

$$\underline{\mathbf{y}} = \bar{\mathbf{A}}(\bar{\mathbf{x}}_Y + \underline{\bar{\mathbf{x}}}_E) + \breve{\mathbf{A}}_Y\breve{\mathbf{x}}_Y + \breve{\mathbf{A}}_E\breve{\mathbf{x}}_E + \underline{\boldsymbol{\epsilon}}_Y + \underline{\boldsymbol{\epsilon}}_E. \tag{8}$$

Assuming normal distributions, it is only necessary to specify the expectation $\mathsf{E}\{.\}$ and variance $\mathsf{var}\{.\}$ of $\underline{\mathbf{y}}$. The chosen models for the expectation and variance of $\underline{\mathbf{y}}$ are often respectively referred to as *functional* and *stochastic* models.

Because $\bar{\mathbf{x}}_\mathrm{E}$ is considered as the realisation of a zero-expectation stochastic variable, the non-stochastic components in the equations for the measured values are $\bar{\mathbf{x}}_Y$, $\breve{\mathbf{x}}_Y$ and $\breve{\mathbf{x}}_E$. Thus, the theoretical functional model of the measured values vector reads

$$\mathsf{E}\{\underline{\mathbf{y}}\} = \mathbf{A}\mathbf{x} = \begin{bmatrix} \bar{\mathbf{A}} & \breve{\mathbf{A}}_Y & \breve{\mathbf{A}}_E \end{bmatrix} \begin{bmatrix} \bar{\mathbf{x}}_Y \\ \breve{\mathbf{x}}_Y \\ \breve{\mathbf{x}}_E \end{bmatrix}, \tag{9}$$

where $\mathbf{A}$ denotes the complete $m \times n$ design matrix and $\mathbf{x}$ denotes the complete $n \times 1$ complete functional parameter vector, with $n$ the number of unknown functional parameters to be estimated. Since the number of common parameters $n_C$ is counted in both $n_Y$ and $n_E$, the total number of estimated functional parameters $n$ can be obtained as $n = n_Y + n_E - n_C$.

The fact that $\bar{\mathbf{x}}_Y$ appears in the unknown functional parameter vector means it is one of the functional parameters that need to be estimated. It does not imply that it can be fully separated from $\bar{\mathbf{x}}_E$. Because of the commonality of their basis functions, the obtained estimate $\widehat{\bar{\mathbf{x}}}_Y$ of $\bar{\mathbf{x}}_Y$ will be the sum of the best-fit values of $\bar{\mathbf{x}}_Y$ and $\bar{\mathbf{x}}_E$. Since $\bar{\mathbf{x}}_E$ is modelled as a stochastic term, its influence on $\widehat{\bar{\mathbf{x}}}_Y$ will be reflected in the uncertainty estimated for $\widehat{\bar{\mathbf{x}}}_Y$.

Assuming the three stochastic components in the extended measured-values equation (namely $\underline{\bar{\mathbf{x}}}_\mathrm{E}$, $\underline{\boldsymbol{\epsilon}}_E$, and $\underline{\boldsymbol{\epsilon}}_Y$) are independent, the variance of the theoretical stochastic model of the measured values vector is

$$\begin{aligned} \mathsf{var}\{\underline{\mathbf{y}}\} = \mathbf{Q}_{\mathbf{y}} &= \mathsf{var}\{\bar{\mathbf{A}}\underline{\bar{\mathbf{x}}}_E\} + \mathsf{var}\{\underline{\epsilon}_E\} + \mathsf{var}\{\underline{\epsilon}_Y\} \\ &= \bar{\mathbf{A}}\mathbf{Q}_{\bar{\mathbf{x}}_E}\bar{\mathbf{A}}^{\top} + \mathbf{Q}_E + \mathbf{Q}_Y, \end{aligned} \tag{10}$$

where $\mathbf{Q}_{\mathbf{y}}$ denotes the complete measurement $m \times m$ covariance matrix (not to be confused with $\mathbf{Q}_Y$).

Though they both refer to measurement errors, the matrices $\bar{\mathbf{A}}\mathbf{Q}_{\bar{\mathbf{x}}_E}\bar{\mathbf{A}}^{\top}$ and $\mathbf{Q}_E$ are kept separated in Eq. (10) to highlight their fundamental difference. While $\mathbf{Q}_E$ could be approximated through empirical (co)variance modelling, $\bar{\mathbf{A}}\mathbf{Q}_{\bar{\mathbf{x}}_E}\bar{\mathbf{A}}^{\top}$ cannot, as the functional-parameter estimates will absorb all its variance during the estimation process due to the collinearity issue (Sect. 3.6). For practical purposes, both matrices could, however, be summed to form a total measurement error covariance matrix $\mathbf{Q}_{TE} = \mathbf{Q}_E + \bar{\mathbf{A}}\mathbf{Q}_{\bar{\mathbf{x}}_E}\bar{\mathbf{A}}^{\top}$, such that

$$\mathsf{var}\{\underline{\mathbf{y}}\} = \mathbf{Q}_{TE} + \mathbf{Q}_Y. \tag{11}$$

### 3.6 Estimating Functional Parameters with Realistic Uncertainties

The unknown parameters of these functional models are grouped in the $n \times 1$ vector of unknowns, denoted by $\mathbf{x}$, which must be estimated through a model fitting procedure. This fitting procedure depends on the estimation principle employed for the analysis. In practice, linear estimators (e.g., ordinary least squares, weighted least squares, generalised least squares, and sometimes maximum-likelihood estimation), are noted $\underline{\hat{\mathbf{x}}}$ and are

$$\underline{\hat{\mathbf{x}}} = \mathbf{G}\underline{\mathbf{y}}, \tag{12}$$

where $\mathbf{G}$ denotes the $n \times m$ matrix associated with the chosen estimator. For instance, when employing GLS estimation, the estimator $\mathbf{G}$ can be written as $\mathbf{G}_{\mathsf{GLS}} = (\mathbf{A}^{\top}\mathbf{Q}_{\mathbf{y}}^{-1}\mathbf{A})^{-1}\mathbf{A}^{\top}\mathbf{Q}_{\mathbf{y}}^{-1}$, whereas when employing OLS estimation $\mathbf{G}$ can be written as $\mathbf{G}_{\mathsf{OLS}} = (\mathbf{A}^{\top}\mathbf{A})^{-1}\mathbf{A}^{\top}$. In Sect. 4, the estimator $\mathbf{G}_{\mathsf{OLS}}$ is used as it is the most frequently used approach, although less statistically efficient than GLS when applied to the same problem. Functional parameter estimates correspond to a realisation $\hat{\mathbf{x}}$ of this estimator $\underline{\hat{\mathbf{x}}}$, obtained from the measured values $\mathbf{y}$ as $\hat{\mathbf{x}} = \mathbf{G}\mathbf{y}$.

The objective of parameter uncertainty assessment is to describe the probability density function (PDF) of parameter estimator $\underline{\hat{\mathbf{x}}}$, which includes the trend estimate. It is performed by propagating the PDFs of the sources of uncertainty through the estimators used to obtain the parameter estimates. For linear(-ised) estimators, and under the normal distribution assumption, parameter estimates follow a multivariate normal distribution, such that PDF propagation simplifies to linear variance propagation.

Thus, the most critical step is to obtain a realistic description of the variance associated with the measured values $\mathbf{y}$, noting $\mathsf{var}\{\underline{\mathbf{y}}\} = \mathbf{Q}_{\mathbf{y}}$, which is challenging because our inventory of the stochastic components can be incomplete, or their statistical description can be oversimplified or erroneous. When a description of $\mathbf{Q}_{\mathbf{y}}$ is available, and when employing a linear estimator $\mathbf{G}$, the covariance matrix of the parameter estimator $\underline{\hat{\mathbf{x}}}$, denoted $\mathbf{Q}_{\hat{\mathbf{x}}}$, can be written as

$$\begin{aligned}\mathsf{var}\{\underline{\hat{\mathbf{x}}}\} = \mathbf{Q}_{\hat{\mathbf{x}}} &= \mathbf{G}\mathbf{Q}_{\mathbf{y}}\mathbf{G}^{\top} \\ &= \mathbf{G}\bar{\mathbf{A}}\mathbf{Q}_{\bar{\mathbf{x}}_E}\bar{\mathbf{A}}^{\top}\mathbf{G}^{\top} + \mathbf{G}\mathbf{Q}_{Y}\mathbf{G}^{\top} + \mathbf{G}\mathbf{Q}_{E}\mathbf{G}^{\top}.\end{aligned} \tag{13}$$

Equation (13) shows that, under the modelling assumptions made above, the functional-parameter uncertainty is the sum of three components, one induced by the uncertainty on the functional components of the measurement errors and two induced by non-functional components of both the measurement errors and the measurand. Depending on the estimator $\mathbf{G}$, different parameter uncertainties are generally obtained corresponding to the parameter estimates provided. According to the Gauss-Markov theorem, the linear estimator resulting in minimal uncertainty is the GLS estimator (Menke 2014).

So far, we have assumed that the functional parameters were estimated using a linear(-ised) estimator. However, for non-linear estimators, the functional parameters are estimated through the application of a nonlinear function or algorithm $f(.)$, such that $\hat{\mathbf{x}} = f(\mathbf{y})$. Employing such estimators will mostly complicate the parameter-uncertainty assessment step. For nonlinear estimators and non-normal distributions, one can use Monte Carlo methods to sample the PDF numerically. Nonetheless, these methods also rely on a realistic description of $\mathbf{Q}_{\mathbf{y}}$ to yield a realistic uncertainty assessment.

### 3.7 Semi-empirical Stochastic Modeling

So far, it has been assumed that the covariance matrix $\mathbf{Q}_{\mathbf{y}}$ is known. However, in many applications, it is at least partly unknown when some of the uncertainty sources are estimated from measured values, using a semi-empirical stochastic model. When prior covariance information is available, such that only part of covariance is unknown, the stochastic model may be divided into a known and a partly unknown part, such that (Teunissen and Amiri-Simkooei 2008)

$$\mathsf{var}\{\underline{\mathbf{y}}\} = \mathbf{Q}_{\mathbf{y}} = \mathbf{Q}_0 + \mathbf{Q}(\boldsymbol{\beta}), \tag{14}$$

where $\mathbf{Q}_0$ denotes the known component of the covariance, and $\mathbf{Q}(\boldsymbol{\beta})$ denotes the part of the covariance that depends on an unknown stochastic parameter vector $\boldsymbol{\beta}$ through a known matrix function $\mathbf{Q}(.)$.

Because it cannot be accounted for otherwise, the known part $\mathbf{Q}_0$ should, at a minimum, include a stochastic description of the functional component of measurement errors that overlaps with that of the measurand, that is $\bar{\mathbf{A}}\hat{\mathbf{Q}}_{\bar{\mathbf{x}}_E}\bar{\mathbf{A}}^{\top}$ in Eq. (10). However, if other information is available, such as the variance matrices of the non-functional part of the measurement error and the measurand, it could also be added to $\mathbf{Q}_0$.

The matrix function $\mathbf{Q}(.)$, which can be empirically motivated or based on previous studies, should compensate for the possible deficiency of $\mathbf{Q}_0$ in describing all the non-functional variations in the measurements. It often describes the covariance matrix of one stochastic process (or a sum of stochastic processes) with unknown variance(s) and structure parameter(s). These parameters can be estimated using variance component estimation methods (Patterson and Thompson 1971; Harville 1977).

Altogether, this semi-empirical stochastic model can account for both prior metrological insights on measurement errors and the lesser-understood and empirically modelled variations. As such, this covariance model can lead to a more complete uncertainty assessment than purely measurement-uncertainty-oriented or

time-series-analysis-oriented approaches. This approach, however, relies on estimating the unknown stochastic-parameter vector $\boldsymbol{\beta}$. This step is explained in Appendix 1.

## 4 Demonstration on the Analysis of a Global Mean Sea Level Time-Series

### 4.1 Introduction to the Sea Level Case Study

Sea level is one of the ECVs identified by the GCOS, and its global mean as a function of time is an important indicator of climate change. Global mean sea level (GMSL) is the global average height of the sea level with respect to a reference surface (Church et al. 2013; Fox-Kemper et al. 2021). Providing an accurate measurement of the temporal evolution of sea level and its global average is a derived product essential for climate change monitoring since it contributes to understanding the energy budget of the Earth system (Chambers et al. 2017; Meyssignac et al. 2019) and predicting the impact of climate change on human communities, particularly in coastal zones (Nicholls and Tol 2006; Mimura 2013).

The current change in GMSL can be accurately measured by satellite altimetry (Nerem 1995; Chelton et al. 2001; Fu and Cazenave 2000; Fu et al. 2009; Egido and Smith 2016). These satellite observations complement that of coastal tide gauges, which have been used to measure local sea levels long before the satellite era (Cipollini et al. 2017; Frederikse et al. 2020). Satellite altimetry missions for measuring GMSL are placed in Low Earth Orbits with ground tracks (trajectories of the sub-satellite point on Earth's surface) repeating about every 10 days. The sea-level measurements obtained from these repeating tracks are then averaged to form a global mean. Since 1993, several altimetry reference missions (TOPEX/Poseidon, Jason 1, Jason 2, Jason 3, Sentinel-6 Michael Freilich) contributed to providing a continuous record of GMSL measurements (Srinivasan and Tsontos 2023), leading to a continuous multi-decadal record, that is still ongoing.

The GMSL time series is most directly used to quantify the rates and acceleration of mean sea level rise globally. For such analyses to be valuable for climate studies, the uncertainties associated with the trend and acceleration must also be documented. This section illustrates the application of the unified uncertainty assessment approach introduced in Sect. 3 to a relatively straightforward time series with importance to climate studies and hazard response.

### 4.2 Data Set

This study uses the GMSL time series, which provides a measured time series $\mathbf{y}$, and an error-covariance matrix describing instrumental uncertainties and uncertainties associated with corrections in the processing of raw measurements to sea level measured values provided by Ablain et al. (2018), which provides a known measurement error covariance matrix, $\mathbf{Q}_0$. The GMSL time series and error-covariance matrix are depicted in Fig. 2. These two products are derived from the first 25 years of sea-level measurements from reference missions between January 1993 and August 2018. Apart from rare exceptions, these products are sampled with a period of 9.91 days, and represent a global spatial and temporal average over that period.

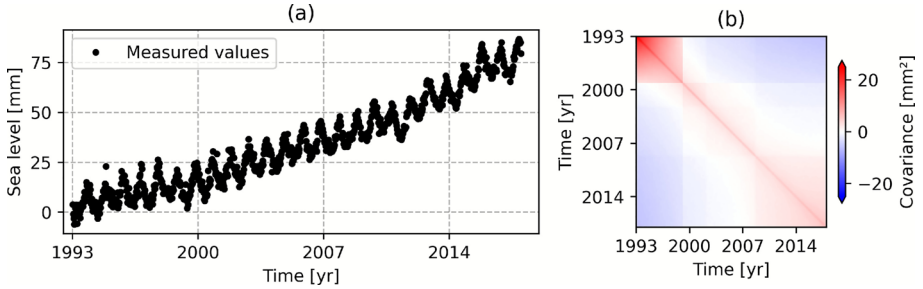


**Fig. 2** Global mean sea-level data set. **a** Time series of the measured values of the GMSL. **b** The covariance matrix associated with the GMSL measurement uncertainties considered by Ablain et al. (2019)

As stated at the beginning of Sect. 3.1, the measured values can be pre-corrected with estimates of undesired variations. Most of these effects are already corrected in the GMSL file provided by AVISO (e.g. ocean tides, atmospherical pressure effects) in order for the GMSL to represent ocean mass and temperature changes only. However, based on Ablain et al. (2018), two additional effects must be also corrected to provide GMSL estimates. First, the GMSL time-series $\mathbf{y}$ is corrected for the linear trend of – 0.3 mm/year induced by the (known and quantifiable) Global Isostatic Adjustment of the Earth's crust. Another effect should be applied to correct instrumental instabilities on TOPEX-A linear drift of – 1.0 mm/year over the 1993.0–1995.5 period and of 3.0 mm/year drift over the 1995.5–1999.2 period (Ablain et al. 2019).

The provided error-covariance matrix $\mathbf{Q}_0$ accounts for uncertainties associated with the GMSL offset estimates between reference missions, the mission-specific drift remaining after the instrumental calibration (altimeter instabilities in TOPEX A and TOPEX B), and certain types of autocorrelated random-measurement and linear-time correlated errors detailed in Ablain et al. (2019). In particular, this matrix $\mathbf{Q}_0$ includes an assessment of the uncertainty induced by the stability of the International Terrestrial Reference Frame (ITRF), which is a typical example of a source of uncertainty that is not estimable from any sea-level measured values due to ITRF's role of reference. Some of these uncertainties were estimated by a number of reasoned investigations, as a metrological end-to-end uncertainty assessment has not yet been fully completed. These estimates of uncertainty will, therefore, likely be refined in the future but are considered sufficiently useful to provide a good estimate of the utility of the uncertainty assessment methodology that is the focus of this study.

### 4.3 Functional and Stochastic Model of the GMSL Time-Series

The time series in Fig. 2 shows a trend with a possible acceleration and a seasonal oscillation. Thus, in this study, we approximate the evolution of global-mean sea level using the model

$$y(t) = y_0 + v(t - t_r) + \frac{a}{2}(t - t_r)^2 + \sum_{i=1}^{3} \left[ c_i \cos(2\pi i f_a (t - t_r)) + s_i \sin(2\pi i f_a (t - t_r)) \right] + e(t), \tag{15}$$

where $y_0$ is the unknown reference value at $t = t_r$, $v$ is the unknown value of long-term linear trend, $a$ is the unknown long-term acceleration, $c_i$ and $s_i$ are the unknown Fourier coefficients of the fundamental annual frequency $f_a$ and two harmonics, and $e(t)$ is a residual term representing non-functional variations. In this demonstration, the (arbitrary) reference date $t_r$ has been chosen as $t_r = 2006.0$, which is the round year closest to the average date.

Denote $\mathbf{x} = [\, y_0,\ v,\ a,\ c_1,\ s_1,\ c_2,\ s_2,\ c_3,\ s_3\, ]^\mathsf{T}$, the unknown functional-parameter vector, and consider the non-functional term $e(t)$ as a zero-expectation random variable. Then the functional model (that is, the expectation of the measured-values vector) can be written as $\mathsf{E}\{\mathbf{y}\} = \mathbf{A}\mathbf{x}$. Without additional information, the stochastic model, which represents the sum of all known stochastic effects, is set by default to be $\mathsf{var}\{\mathbf{y}\} = \mathbf{Q}_\mathbf{y} = \mathbf{Q}_0$, as done in Ablain et al. (2019). We will test the validity of this default stochastic model assumption using the analysis of the post-fit residuals, i.e., the difference between the measured values and the fitted functional model. We use the OLS estimator, as used in Ablain et al. (2019), for the functional-model fitting. The OLS fit is presented in Fig. 3.

### 4.4 Analysis of the Post-fit Residuals

Because the expectation of the functional parameter estimator is, by definition, unknown, it is impossible to judge directly a stochastic model's ability to produce a realistic covariance matrix for parameter estimates. However, since the expectation of the residuals is supposed to be zero, it is possible to evaluate the ability of a stochastic model to describe correctly the covariance matrix of the residuals. The motivation for doing so is that a stochastic model that poorly describes the covariance matrix of the residuals might also poorly predict the covariance matrix of the functional parameter estimates. Consequently, the analysis of residuals can be viewed as an indirect method

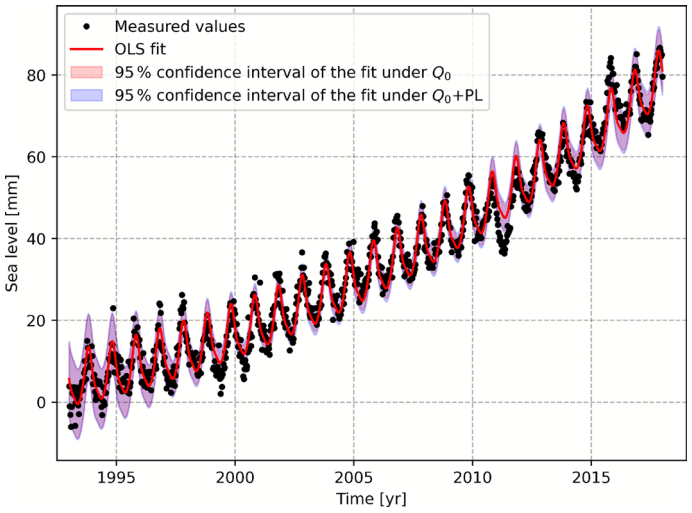


**Fig. 3** Ordinary least-squares fit of the measurement model in expression (15) and its 95% confidence interval under the $Q_0$ model (red confidence band) and the $Q_0$+PL model (blue confidence band)

for stochastic model validation. In our context, we expect that the provided error covariance matrix $\mathbf{Q}_0$ alone does not fully explain all the variations in the residuals. So instead of validating $\mathbf{Q}_0$, this residual analysis will help determine to which extent it should be empirically completed by covariance term $\mathbf{Q}(\boldsymbol{\beta})$.

Residuals can be analysed in various ways. In this study, we assess the ability of the selected stochastic model and the provided matrix $\mathbf{Q}_0$ in particular to describe both the dispersion and the power spectrum of residuals calculated using the OLS fitting of Eq. (15) on the data.

The time series of the estimated residuals, denoted by $\widehat{\mathbf{e}}$, and its predicted covariance matrix $\mathbf{Q}_{\widehat{\mathbf{e}}}$, can be computed as

$$\begin{aligned} \widehat{\mathbf{e}} &= \mathbf{y} - \mathbf{A}\widehat{\mathbf{x}}, \\ \mathbf{Q}_{\widehat{\mathbf{e}}} &= (\mathbf{I} - \mathbf{AG})\mathbf{Q}_{\mathbf{y}}(\mathbf{I} - \mathbf{AG})^{\top}, \end{aligned} \tag{16}$$

where $\widehat{\mathbf{x}}$ is the estimated functional parameter vector and $\mathbf{G}$ is the functional parameter estimator (Eq. (12)), which here is the OLS estimator for comparability with Ablain et al. (2019).

The estimated post-fit residuals are presented in black in Fig. 4. The predicted 95% confidence interval for the residuals is obtained from the diagonal elements of $\mathbf{Q}_{\widehat{\mathbf{e}}}$ calculated assuming $\mathbf{Q}_{\mathbf{y}} = \mathbf{Q}_0$ in Eq. (16). This confidence interval is depicted in red (inner uncertainty band), in Fig. 4. 20.0% of the residuals fall outside the 95% confidence interval, showing that $\mathbf{Q}_0$, which solely characterises measurement errors, needs to be completed with empirical stochastic modelling to capture the remaining non-functional variations due to global mean sea level and possibly non-budgeted measurement errors.

Besides dispersion, to obtain additional insight into the temporal structure of the non-functional variations described by $\mathbf{Q}_0$ in the data, we study its prediction for the shape of the residuals' Lomb-Scargle power spectrum (Vaníček 1969; Lomb 1976; Scargle 1982). To compute the confidence intervals for the Lomb-Scargle power spectrum, we apply a

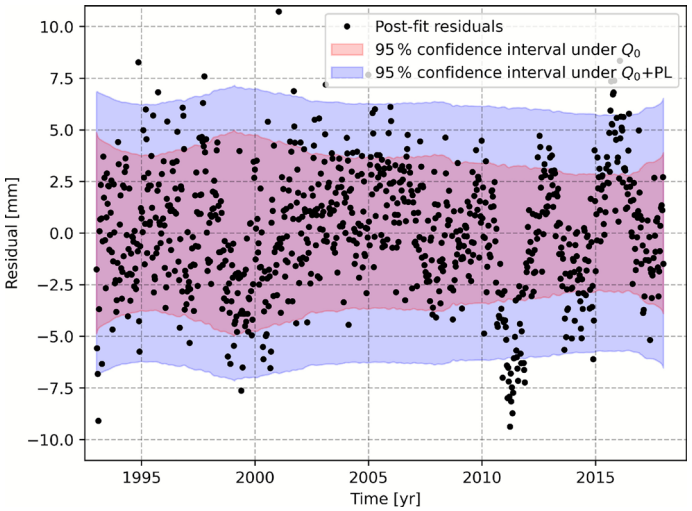


**Fig. 4** Time series of the OLS post-fit residuals (black solid line), and the predicted confidence interval using the $\mathbf{Q}_0$ model (inner, red, shaded area), and the $\mathbf{Q}_0$+PL model (outer, blue, shaded area)

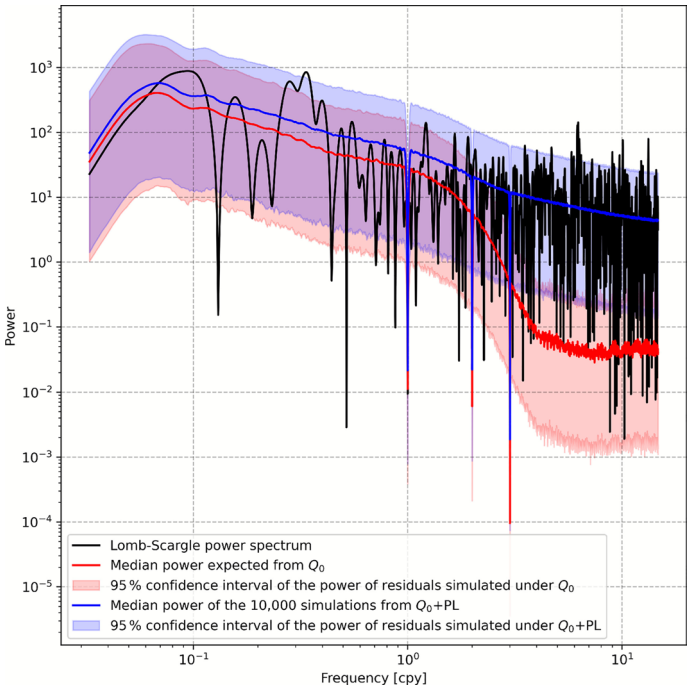


**Fig. 5** Lomb-Scargle power spectrum of the OLS post-fit residuals (black solid line), and the associated medians (solid lines) and 95% confidence intervals (shaded areas) derived from residuals simulated with the $\mathbf{Q}_0$ model (red) and the $\mathbf{Q}_0$+PL model (blue)

Monte Carlo approach. First, we sample 10 000 time-series from the predicted $\mathcal{N}(\mathbf{0}, \mathbf{Q}_{\hat{\mathbf{e}}})$ distribution. Then, for each frequency, we define the 95% confidence interval in terms of its endpoints, the 2.5% and 97.5% quantiles of the distribution of spectral powers calculated from these 10 000 samples. The power spectrum of the residuals is presented in black in Fig. 5. The predicted 95% confidence interval is shown in red. This analysis suggests that the provided error covariance matrix $\mathbf{Q}_0$ may almost explain residual variations below 1.0 cycle per year (cpy), but it needs to be completed to describe the shorter-term variations in the time-series, namely those above 2.0 cpy.

### 4.5 Augmented Stochastic Model

The power spectrum of the residual displays a slope on log-log scales (Fig. 5), rather than the flat output that would be expected for pure white noise, suggesting that part of the non-functional variations could be better described by a power-law stochastic process (Mandelbrot and Van Ness 1968). Thus, to complete the *a priori* stochastic model, we consider the following augmented stochastic model:

$$\mathsf{var}\{\mathbf{y}\} = \mathbf{Q}_0 + \gamma \mathbf{Q}_{\mathrm{PL}}(\kappa), \tag{17}$$

where $\gamma$ denotes the unknown variance factor of a power-law process, $\mathbf{Q}_{\mathrm{PL}}$ denotes the cofactor matrix of the power-law process, which depends on $\kappa$, the unknown spectral index

of the process (Hosking 1981; Williams 2003). In the following, this model is called the $Q_0$ +PL model.

The unknown power-law process parameters, namely, $\gamma$ and $\kappa$, are estimated using the restricted maximum-likelihood estimation method (Appendix 1). For better interpretability, the covariance matrix $\mathbf{Q}_{\mathrm{PL}}(\kappa)$ was scaled so that $\gamma$ can be interpreted as the expected empirical variance over the observation period, in mm$^2$, following Gobron et al. (2021). The best-fitting stochastic parameters are $\widehat{\gamma} = 7.20$ mm$^2$ and $\widehat{\kappa} = -0.74$. The $Q_0$+PL model's predictions for the dispersion of the residuals are presented in blue in Fig. 4, whereas its predictions for the power-spectral values are shown in blue in Fig. 5. With this correction, only 3.8% of the residuals fall outside the predicted 95% confidence interval (Fig. 4). The improvement in dispersion description is even more visible in Fig. 6, which presents the quantile-quantile plots of the residuals normalised using the residuals' covariance derived using the $Q_0$ and $Q_0$+PL models. Such a better agreement in Fig. 6 is nonetheless anticipated since the parameters $\gamma$ and $\kappa$ were indirectly optimised to reflect these quantiles better. Besides dispersion, the high-frequency variations are now more realistically modelled (Fig. 5). The estimated functional parameters and the uncertainty derived from the $Q_0$ and $Q_0$+PL models are presented in Table 1. Appendix 2 presents the corresponding parameter uncertainty correlations. The change in uncertainty and correlations is most visible for parameters describing higher-frequency effects, and particularly seasonal effects. The influence of the change in uncertainty on the confidence interval of the fitted functional model is illustrated in

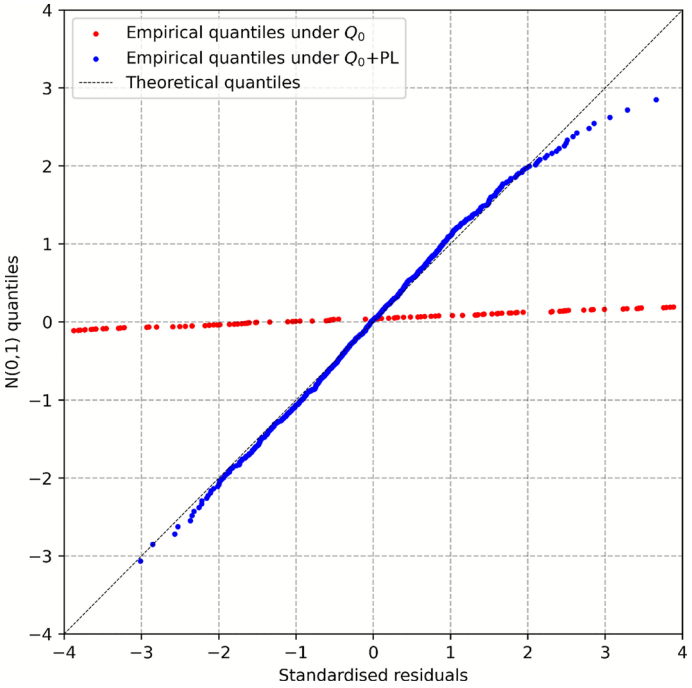


**Fig. 6** Quantile-quantile plots of the residuals standardised using the residuals' covariance estimated using the $Q_0$ model (red dots) and the $Q_0$+PL model (blue dots). The empirical quantiles should ideally lie along the dashed black line

**Table 1** Estimated functional parameters and their associated standard uncertainties $u(.)$ under the $Q_0$ and $Q_0$+PL models

| Parameter | Unit | Estimate | $u(\mathbf{Q}_0)$ | $u(\mathbf{Q}_0 + \mathrm{PL})$ |
|---|---|---|---|---|
| $y_0$ | mm | 32.093 | 1.195 | 1.574 |
| $v$ | mm/year | 3.043 | 0.220 | 0.232 |
| $a$ | mm/year$^2$ | 0.142 | 0.044 | 0.048 |
| $c_1$ | mm | 3.241 | 0.209 | 0.289 |
| $s_1$ | mm | − 5.311 | 0.209 | 0.291 |
| $c_2$ | mm | − 1.124 | 0.094 | 0.182 |
| $s_2$ | mm | − 0.951 | 0.094 | 0.183 |
| $c_3$ | mm | − 0.396 | 0.027 | 0.137 |
| $s_3$ | mm | − 0.080 | 0.030 | 0.138 |

Fig. 3. The specific impact of the stochastic model improvement on the estimated trend uncertainties is discussed in more detail in the following section.

### 4.6 Impact on the Estimated Trend Uncertainties

The uncertainty associated with trend estimates depends on the period over which the trend is evaluated. To provide a more detailed uncertainty description, Ablain et al. (2019) introduced an uncertainty triangle representing trend uncertainty as a function of a central date and a period length. This section thus investigates the impact of the stochastic-model definition on these uncertainty triangles.

Figure 7 presents the uncertainty triangle calculated using the $Q_0$ stochastic model alongside that calculated using the $Q_0$+PL model. The relative uncertainty change, expressed as a percentage, is also presented in Fig. 7. The uncertainty differences between the $Q_0$ and $Q_0$+PL models are minimal for the longest period lengths (above 20 years), and the increase with the $Q_0$+PL model is only 5.1% for the maximum period (25 years). The increase is small because, in this GMSL example, the low-frequency component of the $Q_0$ +PL model is dominated by the provided measurement-error covariance matrix $Q_0$ (see Fig. 5). However, for shorter periods, the relative change in uncertainty between the two stochastic models is larger and reaches a maximum of 60.7% for the 1.0 year period length. These observed changes highlight the utility of the empirical stochastic modelling to provide self-consistent estimates of uncertainty across a range of time scales.

### 4.7 Summary of the GMSL Demonstration

Building upon the theoretical developments of Sect. 3, this demonstration section explains how to combine available covariance information regarding measurement uncertainty with empirical stochastic modelling for practical trend uncertainty assessment. In the context of a global mean sea level study, this demonstration first highlights that the crucial measurement uncertainty information provided by Ablain et al. (2019), especially regarding long-term stability uncertainty, can be assimilated in the form of a known covariance matrix $\mathbf{Q}_0$. Then, this demonstration demonstrates how empirical stochastic modelling can help improve the description of the post-fit residuals, which leads to less optimistic trend uncertainties. In this demonstration, the uncertainty change for the longest period is small because the provided covariance matrix $\mathbf{Q}_0$ explains well low-frequency

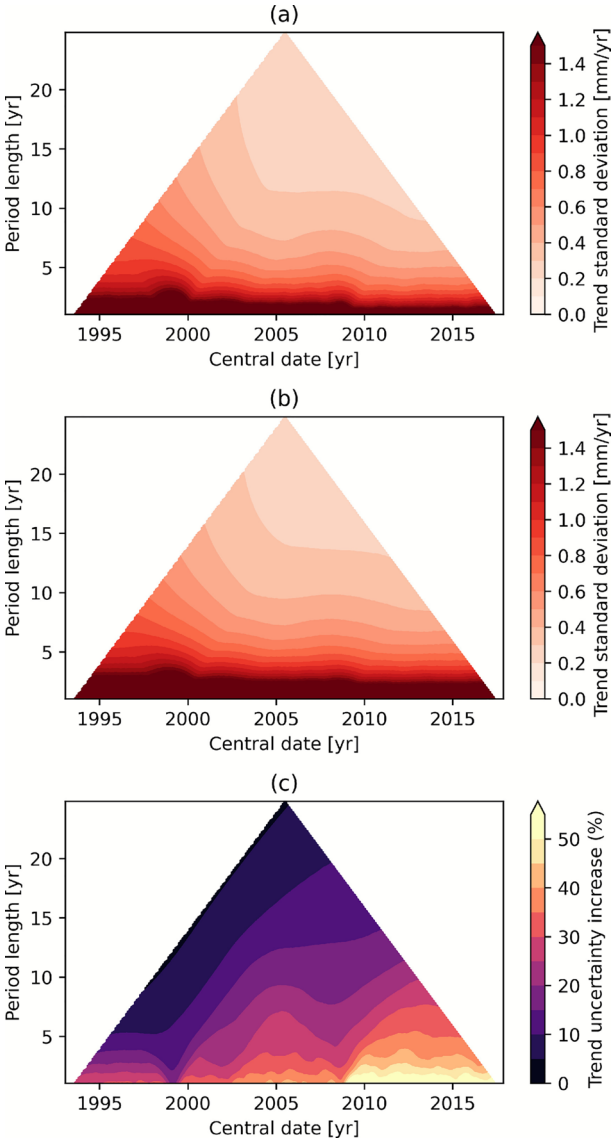


**Fig. 7** **a** Trend standard uncertainty under the $Q_0$ stochastic model. **b** Trend standard uncertainty under the $Q_0$+PL stochastic model. **c** Change in standard uncertainty resulting from the change of stochastic model

effects. For other applications, with possibly less complete error covariance information, more significant changes in trend uncertainty could be expected for all period lengths after empirical stochastic modelling.

Although this section demonstrates an improvement in uncertainty assessment, the statistical modelling of the GMSL time series could see further improvement in the future.

Firstly, an improved error covariance matrix could be provided to better separate the effects due to pure measurement errors from those due to natural oceanic variability (e.g. mesoscale circulation). Second, we did not attempt to model the extreme deviations of sea level from the long-term behaviour, which are very well correlated to El Niño–Southern Oscillation events (e.g., Piecuch and Quinn 2016). Nevertheless, these events should be the subject of dedicated functional or stochastic modelling. However, finding an appropriate modelling approach is beyond this study's scope.

## 5 Conclusion and Outlook

Attributing realistic uncertainties to trends estimated from climate data records is essential for rigorously interpreting the observed changes. It is especially critical for analysing subtle trends, which are of major interest in understanding climate change. However, despite the importance of uncertainty, no established trend uncertainty-assessment approach properly accounts for all known sources of trend uncertainty. Most approaches neglect parts of known measurement uncertainty, such as measurement system instability, or ignore the influence of natural climate variability on trend estimation. In this study, we addressed several known limitations of existing uncertainty-assessment approaches, proposing an improved approach and demonstrating its application to analysing a global mean sea-level time series.

To overcome this methodological limitation, Sect. 3 presented an alternative view of uncertainty assessment and proposed an alternative strategy, combining available metrological information with empirical time-series analysis. Empirical modelling allowed us to account for the measurand's non-functional variations and compensate for the possible deficiencies of the measurement-uncertainty information in describing non-functional measurement errors. This alternative approach was applied, as a proof of concept, to the modelling of the Global Mean Sea Level time series in Sect. 4. This application demonstrated that complementing measurement uncertainty information with empirical modelling can notably improve trend uncertainty assessment.

While the proposed uncertainty-assessment approach constitutes a notable improvement over current practice, it could be improved further. In particular, the approach neglects the fact that the functional model may be partly retrieved from measurements, such as through a combination of estimation and hypothesis testing. In such a case, the estimation procedure is nonlinear, which could lead to a more complex distribution of parameter estimates (Teunissen 2018). This uncertainty estimation approach also does not consider that stochastic parameters are estimates subject to uncertainty. This fact also complicates uncertainty estimation in a way that remains to be quantified, which will be the subject of future investigations. For simplicity, this study focused on the temporal domain. In practice, many geoscientific applications use an ensemble of trends or parameters estimated around the globe as input. When dealing with quantities estimated at different locations, it is necessary to account additionally for the spatial structure of the measurand and measurement errors. Future work is, therefore, necessary to move toward providing a spatio-temporal description of covariance of the stochastic term in the measured values.

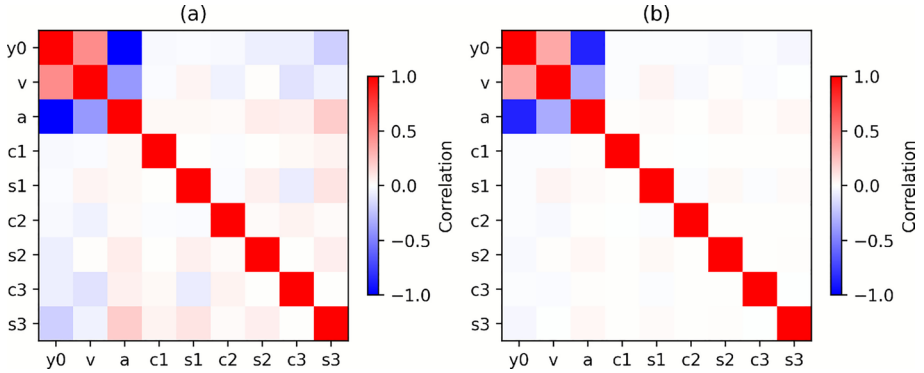


**Fig. 8** **a** Correlation matrix of the functional parameter estimate uncertainties under the $Q_0$ model. **b** As (a), but under the $Q_0$+PL model

## Appendix 1: Variance Component Estimation

The statistical methods devoted to estimating stochastic parameters are called variance-component estimation (VCE) methods. A wide variety of VCE methods have been developed over recent decades. Detailing these methods is beyond the scope of this paper, and the reader may refer to chapter 3 of Amiri Simkooei (2007) for a review.

Under the multivariate normal-distribution assumption, an unbiased and minimum-variance estimate of $\widehat{\boldsymbol{\beta}}$ in Eq. (14) can be achieved by maximising the restricted log-likelihood $\ln(\mathcal{L}_R(\mathbf{y} \mid \boldsymbol{\beta}))$:

$$\widehat{\boldsymbol{\beta}} = \underset{\boldsymbol{\beta}}{\operatorname{argmax}} \ln(\mathcal{L}_R(\mathbf{y} \mid \boldsymbol{\beta})), \tag{18}$$

where $\ln(\mathcal{L}_R(\mathbf{y} \mid \boldsymbol{\beta}))$ can be computed as in Harville (1977):

$$\begin{aligned} \ln(\mathcal{L}_R(\mathbf{y} \mid \boldsymbol{\beta})) = -\frac{1}{2}[&(m-n)\ln(2\pi) \\ &+ \ln(\det(\mathbf{A}^\top \mathbf{Q}_{\mathbf{y}}^{-1}(\boldsymbol{\beta})\mathbf{A})) \\ &+ \ln(\det(\mathbf{Q}_{\mathbf{y}}(\boldsymbol{\beta}))) + \widehat{\mathbf{e}}^\top \mathbf{Q}_{\mathbf{y}}^{-1}(\boldsymbol{\beta})\widehat{\mathbf{e}}] + c, \end{aligned} \tag{19}$$

in which $c$ is a term that does not depend on $\boldsymbol{\beta}$ and can be ignored for variance-component estimation.

Once the parameter estimates $\widehat{\boldsymbol{\beta}}$ is obtained, using a numerical maximization algorithm, an estimated total covariance matrix can be constructed as $\widehat{\mathbf{Q}}_{\mathbf{y}} = \mathbf{Q}_0 + \mathbf{Q}(\widehat{\boldsymbol{\beta}})$. This estimated covariance matrix should be more realistic than $\mathbf{Q}_0$ alone and can be used for functional parameter uncertainty assessment.

## Appendix 2: Correlation Matrix of Functional Parameter Estimate Uncertainties

Besides causing a change in uncertainty, employing the augmented stochastic model $Q_0$ +PL changes the correlation between functional parameter estimate uncertainties. This effect is illustrated in Fig. 8, where notable changes in the correlations for the periodic parameter estimates can be observed. These correlation changes mostly emphasize the relative influence of $\mathbf{Q}_0$ and $\gamma\mathbf{Q}_{\mathrm{PL}}(\kappa)$ in the augmented model, already observed in Table 1.

**Acknowledgements** This paper is an outcome of the Workshop 'Remote Sensing in Climatology: Essential Climate Variables and their Uncertainties' held at the International Space Science Institute (ISSI) in Bern, Switzerland (13-17 November 2023). Contributions to this paper were supported by the national capability funding for the National Centre for Earth Observation from the Natural Environment Research Council through award NE/R016518/1. For the purpose of open access, the authors have applied a Creative Commons Attribution (CC BY) licence to the Author Accepted Manuscript version arising from this submission. Kevin Gobron is grateful to the Centre National d'Étude Spatiales (CNES) for the postdoctoral fellowship that allowed him to contribute to this work. The input from the National Physical Laboratory was supported by the National Measurement System programme of the UK Government's Department for Science, Innovation and Technology. Anna Klos and Janusz Bogusz are supported by the National Science Center (Poland), grant no. UMO-2022/45/B/ST10/00333.

**Author contributions** All authors defined this study's research objectives during discussions held at the 'Remote Sensing in Climatology: Essential Climate Variables and their Uncertainties' International Space Science Institute workshop in Bern or the following meetings. A main writing team composed of KG, RH, XL, CEB, CJM, and ERW prepared the initial manuscript draft with complementary inputs from all authors. The authors of this main writing team are ordered based on an estimate of their relative contributions to the construction of this initial draft. The initial manuscript draft was then improved based on complete reviews carried out by a second group of authors composed of MGC, WD, TH, ML, and ACP. Finally, throughout the writing process, a third group of authors, composed of MA, JB, AG, AK, and JM, also provided input on specific topics. For simplicity, the authors of the second and third groups are listed in alphabetic order within their group.

**Data availability** The data used to produce this work is available at https://doi.org/10.17882/58344. The codes used to produce the results presented in this study will be accessible at the following Zenodo repository: https://doi.org/10.5281/zenodo.15387896. These codes are also available upon request.

## Declarations

**Conflict of interest** All authors declare that they have no conflict of interest.

## References


Ablain M, Meyssignac B, Zawadzki L, et al (2018) Error variance-covariance matrix of global mean sea level estimated from satellite altimetry (TOPEX, Jason 1, Jason 2, Jason 3). Sea Scientific Open Data Publication https://doi.org/10.17882/58344

Ablain M, Meyssignac B, Zawadzki L et al (2019) Uncertainty in satellite estimates of global mean sea-level changes, trend and acceleration. Earth Syst Sci Data 11(3):1189–1202. https://doi.org/10.5194/essd-11-1189-2019

Agnew DC (1992) The time-domain behavior of power-law noises. Geophys Res Lett 19(4):333–336. https://doi.org/10.1029/91GL02832

Amiri Simkooei A (2007) Least-squares variance component estimation: Theory and gps applications. Dissertation (tu delft), Delft University of Technology

Arguez A, Yu P, O'Brien JJ (2008) A new method for time series filtering near endpoints. J Atmos Oceanic Tech 25(4):534–546. https://doi.org/10.1175/2007JTECHA924.1

Bevis M, Bedford J, Caccamise DJ (2020) The art and science of trajectory modelling. In: Montillet J, Bos M (eds) Geodetic time series analysis in earth sciences. Springer, Cham, pp 1–27. https://doi.org/10.1007/978-3-030-21718-1_1

BIPM, IEC, IFCC, et al (2008) Evaluation of measurement data—Guide to the expression of uncertainty in measurement. Joint Committee for Guides in Metrology, JCGM 100:2008. https://doi.org/10.59161/JCGM100-2008E

BIPM, IEC, IFCC, et al (2012) International Vocabulary of Metrology—Basic and general concepts and associated terms (VIM). Joint Committee for Guides in Metrology, JCGM 200:2012. (3rd edition). https://doi.org/10.59161/JCGM200-2012

BIPM, IEC, IFCC, et al (2020) Guide to the expression of uncertainty in measurement—Part 6: Developing and using measurement models. Joint Committee for Guides in Metrology, JCGM GUM-6:2020. https://doi.org/10.59161/jcgmgum-6-2020

Boergens E, Kvas A, Eicker A et al (2022) Uncertainties of grace-based terrestrial water storage anomalies for arbitrary averaging regions. J Geophys Res Solid Earth 127(2):e2021JB022081. https://doi.org/10.1029/2021JB022081

Bos M, Williams S, Araújo I et al (2014) The effect of temporal correlated noise on the sea level rate and acceleration uncertainty. Geophys J Int 196(3):1423–1430. https://doi.org/10.1093/gji/ggt481

Brockwell PJ, Davis RA (2002) Introduction to time series and forecasting. Springer. https://doi.org/10.1007/978-3-319-29854-2

Bulgin C, Mittaz J, Embury O et al (2018) Bayesian cloud detection for 37 years of Advanced Very High Resolution Radiometer (AVHRR) Global Area Coverage data. Remote Sens. https://doi.org/10.3390/rs10010097

Bulgin CE, Maidment RI, Ghent D et al (2024) Stability of cloud detection methods for Land Surface Temperature (LST) Climate Data Records (CDRs). Remote Sens Environ. https://doi.org/10.1016/j.rse.2024.114440

Bulgin CE, Green P, Gruber A et al (2025) The importance of scale in the definition of uncertainties: How do we best communicate this to data users? Surv Geophys. https://doi.org/10.1007/s10712-025-09908-5

Chambers DP, Cazenave A, Champollion N, et al (2017) Evaluation of the global mean sea level budget between 1993 and 2014. Integrative study of the mean sea level and its components, pp 315–333. https://doi.org/10.1007/978-3-319-56490-6_14

Chelton DB, Ries JC, Haines BJ, et al (2001) Satellite altimetry. In: International geophysics, vol 69. Elsevier, pp 1–ii. https://doi.org/10.1016/S0074-6142(01)80146-7

Christy JR, Spencer RW, Braswell WD (2000) MSU tropospheric temperatures: dataset construction and radiosonde comparisons. J Atmos Oceanic Tech 17(9):1153–1170. https://doi.org/10.1175/1520-0426(2000)0172.0.CO;2

Church J, Clark P, Cazenave A, et al (2013) Sea level change: Chapter 13. In: The Physical Science Basis: Contribution of Working Group I to the Fifth Assessment Report of the Intergovernmental Panel on Climate Change. Cambridge University Press

Cipollini P, Calafat FM, Jevrejeva S, et al (2017) Monitoring sea level in the coastal zone with satellite altimetry and tide gauges. Integrative study of the mean sea level and its components, pp 35–59. https://doi.org/10.1007/978-3-319-56490-6_3

Davis J, Wernicke B, Tamisiea M (2012) On seasonal signals in geodetic time series. J Geophys Res Solid Earth. https://doi.org/10.1029/2011JB008690

de La Serve M, Rebischung P, Collilieux X et al (2023) Are there detectable common aperiodic displacements at ITRF co-location sites? J Geod 97(8):79. https://doi.org/10.1007/s00190-023-01769-3

Deser C, Knutti R, Solomon S et al (2012) Communication of the role of natural variability in future north american climate. Nat Clim Chang 2:775–779. https://doi.org/10.1038/nclimate1562
Deser C, Phillips A, Bourdette V et al (2012) Uncertainty in climate change projections: the role of internal variability. Clim Dyn 38:527–546. https://doi.org/10.1007/s00382-010-0977-x
Dieng HB, Cazenave A, Meyssignac B et al (2017) New estimate of the current rate of sea level rise from a sea level budget approach. Geophys Res Lett 44(8):3744–3751. https://doi.org/10.1002/2017GL073308
Dong D, Fang P, Bock Y et al (2002) Anatomy of apparent seasonal variations from gps-derived site position time series. J Geophys Res Solid Earth. https://doi.org/10.1029/2001JB000573
Dorigo W, de Jeu R, Chung D et al (2012) Evaluating global trends (1988–2010) in harmonized multi-satellite surface soil moisture. Geophys Res Lett. https://doi.org/10.1029/2012GL052988
Dorigo W, Dietrich S, Aires F et al (2021) Closing the water cycle from observations across scales: where do we stand? Bull Am Meteorol Soc 102(10):E1897–E1935. https://doi.org/10.1175/BAMS-D-19-0316.1
Egido A, Smith WH (2016) Fully focused SAR altimetry: theory and applications. IEEE Trans Geosci Remote Sens 55(1):392–406. https://doi.org/10.1109/TGRS.2016.2607122
Embury O, Merchant C, Good S et al (2024) Satellite-based time-series of sea-surface temperature since 1980 for climate applications. Sci Data. https://doi.org/10.1038/s41597-019-0236-x
Eyring V, Bony S, Meehl GA et al (2016) Overview of the Coupled Model Intercomparison Project Phase 6 (CMIP6) experimental design and organization. Geosci Model Dev 9(5):1937–1958. https://doi.org/10.5194/gmd-9-1937-2016
Fernandes R, LeBlanc SG (2005) Parametric (modified least squares) and non-parametric (Theil-Sen) linear regressions for predicting biophysical parameters in the presence of measurement errors. Remote Sens Environ. https://doi.org/10.1016/j.rse.2005.01.005
Folland CK, Rayner NA, Brown S et al (2001) Global temperature change and its uncertainties since 1861. Geophys Res Lett 28(13):2621–2624. https://doi.org/10.1029/2001GL012877
Fox-Kemper B, Hewitt HT, Xiao C, et al (2021) Ocean, cryosphere, and sea level change. In: Climate Change 2021: The Physical Science Basis. Contribution of Working Group I to the Sixth Assessment Report of the Intergovernmental Panel on Climate Change. Cambridge University Press, pp 1211–1361
Franzke C (2012) Nonlinear trends, long-range dependence, and climate noise properties of surface temperature. J Clim 25(12):4172–4183. https://doi.org/10.1175/JCLI-D-11-00293.1
Frederikse T, Landerer F, Caron L et al (2020) The causes of sea-level rise since 1900. Nature 584(7821):393–397. https://doi.org/10.1038/s41586-020-2591-3
Fu LL, Cazenave A (2000) Satellite altimetry and earth sciences: a handbook of techniques and applications. Elsevier
Fu LL, Alsdorf D, Rodriguez E et al (2009) The SWOT (Surface Water and Ocean Topography) mission: Spaceborne radar interferometry for oceanographic and hydrological applications. Proc OCEANOBS 9:21–25
Ghent D, Veal K, Trent T et al (2019) A new approach to defining uncertainties for MODIS land surface temperature. Remote Sens. https://doi.org/10.3390/rs11091021
Ghil M (2002) Natural climate variability. Encyclopedia Glob Environ Change 1:544–549
Ghil M, Vautard R (1991) Interdecadal oscillations and the warming trend in global temperature time series. Nature 350(6316):324–327. https://doi.org/10.1038/350324a0
Ghil M, Allen MR, Dettinger MD et al (2002) Advanced spectral methods for climatic time series. Rev Geophys 40(1):3–1. https://doi.org/10.1029/2000RG000092
Gobron K, Rebischung P, Van Camp M et al (2021) Influence of aperiodic non-tidal atmospheric and oceanic loading deformations on the stochastic properties of global GNSS vertical land motion time series. J Geophys Res Solid Earth 126(9):e2021JB022370. https://doi.org/10.1029/2021JB022370
Good E, Aldred F, Ghent D et al (2022) An analysis of the stability and trends in the LST_cci land surface temperature datasets over Europe. Earth Space Sci. https://doi.org/10.1029/2022EA002317
Good S, Fiedler E, Mao C et al (2020) The current configuration of the OSTIA system for the operational production of foundation sea surface temperature and ice concentration analyses. Remote Sens. https://doi.org/10.3390/rs12040720
Granger CW, Joyeux R (1980) An introduction to long-memory time series models and fractional differencing. J Time Ser Anal 1(1):15–29. https://doi.org/10.1111/j.1467-9892.1980.tb00297.x
Hamed KH, Rao AR (1998) A modified mann-kendall trend test for autocorrelated data. J Hydrol 204(1–4):182–196. https://doi.org/10.1016/S0022-1694(97)00125-X

Harris P, Sotirakopoulos K, Robinson S et al (2019) A statistical method for the evaluation of long term trends in underwater noise measurements. J Acoust Soc Am 145(1):228–242. https://doi.org/10.1121/1.5084040

Harville DA (1977) Maximum likelihood approaches to variance component estimation and to related problems. J Am Stat Assoc 72(358):320–338. https://doi.org/10.2307/2286796

Hawkins E, Sutton R (2009) The potential to narrow uncertainty in regional climate predictions. Bull Am Meteorol Soc 90(8):1095–1107. https://doi.org/10.1175/2009BAMS2607.1

Hegerl G, Zwiers F (2011) Use of models in detection and attribution of climate change. Wiley Interdiscip Rev Clim Change 2(4):570–591. https://doi.org/10.1002/wcc.121

Hirsch RM, Slack JR (1984) A nonparametric trend test for seasonal data with serial dependence. Water Resour Res 20(6):727–732. https://doi.org/10.1029/WR020i006p00727

Hirsch RM, Slack JR, Smith RA (1982) Techniques of trend analysis for monthly water quality data. Water Resour Res 18(1):107–121. https://doi.org/10.1029/WR018i001p00107

Hirschi M, Stradiotti P, Crezee B et al (2025) Potential of long-term satellite observations and reanalysis products for characterising soil drying: trends and drought events. Hydrol Earth Syst Sci 29:397–425. https://doi.org/10.5194/hess-29-397-2025

Hosking JRM (1981) Fractional differencing. Biometrika 68(1):165–176. https://doi.org/10.2307/2335817

Huang NE, Shen Z, Long SR et al (1998) The empirical mode decomposition and the hilbert spectrum for nonlinear and non-stationary time series analysis. Proceedings of the Royal Society of London. Series A: Mathematical, Physical and Engineering Sciences 454(1971):903–995. https://doi.org/10.1098/rspa.1998.0193

Hughes CW, Williams SD (2010) The color of sea level: Importance of spatial variations in spectral shape for assessing the significance of trends. J Geophys Res Oceans. https://doi.org/10.1029/2010JC006102

Humphrey V, Gudmundsson L, Seneviratne SI (2016) Assessing global water storage variability from grace: trends, seasonal cycle, subseasonal anomalies and extremes. Surv Geophys 37(2):357–395

Intergovernmental Panel on Climate Change (2021) Technical summary. In: Masson-Delmotte V, Zhai P, Pirani A, et al (eds) Climate Change 2021: The Physical Science Basis. Contribution of Working Group I to the Sixth Assessment Report of the Intergovernmental Panel on Climate Change. Cambridge University Press, pp 33–144. https://www.ipcc.ch/report/ar6/wg1/

ISO (2017) ISO 21748. Guidance for the use of repeatability, reproducibility and trueness estimates in measurement uncertainty evaluation. International Standards Organization, Geneva

Kendall MG (1955) Rank correlation methods. Griffin

Klos A, Olivares G, Teferle FN et al (2018) On the combined effect of periodic signals and colored noise on velocity uncertainties. GPS Solut. https://doi.org/10.1007/s10291-017-0674-x

Langsdale M, Verhoelst T, Povey A et al (2025) The challenges and limitations of validating satellite-derived datasets using independent measurements: lessons learned from essential climate variables. Surv Geophys. https://doi.org/10.1007/s10712-025-09898-4

Li Z, Zhao X, Kahn R et al (2009) Uncertainties in satellite remote sensing of aerosols and impact on monitoring its long-term trend: a review and perspective. Ann Geophys 27(7):2755–2770. https://doi.org/10.5194/angeo-27-2755-2009

Lobell DB, Schlenker W, Costa-Roberts J (2011) Climate trends and global crop production since 1980. Science 333(6042):616–620. https://doi.org/10.1126/science.1204531

Lomb NR (1976) Least-squares frequency analysis of unequally spaced data. Astrophys Space Sci 39(2):447–462. https://doi.org/10.1007/BF00648343

Maher N, Lehner F, Marotzke J (2020) Quantifying the role of internal variability in the temperature we expect to observe in the coming decades. Environ Res Lett 15(5):054014. https://doi.org/10.1088/1748-9326/ab7d02

Mandelbrot BB, Van Ness JW (1968) Fractional Brownian motions, fractional noises and applications. SIAM Rev 10(4):422–437

Mann HB (1945) Nonparametric tests against trend. Econometrica 13(3):245–259. https://doi.org/10.2307/1907187

Mann ME (2004) On smoothing potentially non-stationary climate time series. Geophys Res Lett. https://doi.org/10.1029/2004GL019569

Mann ME (2008) Smoothing of climate time series revisited. Geophys Res Lett. https://doi.org/10.1029/2008GL034716

Meehl GA, Stocker TF, Collins WD, et al (2007) Global Climate Projections. In: Solomon S, Qin D, Manning M, et al (eds) Climate Change 2007: The Physical Science Basis. Contribution of Working Group I to the Fourth Assessment Report of the Intergovernmental Panel on Climate Change.

Cambridge University Press, Cambridge, UK and New York, NY, USA, pp 747–845. https://www.ipcc.ch/report/ar4/wg1/
Menke W (2014) Review of the generalizd least squares method. Surv Geophys 36:1–25. https://doi.org/10.1007/s10712-014-9303-1
Merchant C, et al (2026) Stability specifications for climate data records: their meaning and application in evaluating geophysical trend uncertainty. (In review at Surveys in Geophysics for publication in this special issue).
Merchant CJ, Paul F, Popp T et al (2017) Uncertainty information in climate data records from Earth observation. Earth System Science Data 9(2):511–527. https://doi.org/10.5194/essd-9-511-2017
Merchant CJ, Allan RP, Embury O (2025) Quantifying the acceleration of multidecadal global sea surface warming driven by earth's energy imbalance. Environ Res Lett. https://doi.org/10.1088/1748-9326/adaa8a
Meyssignac B, Boyer T, Zhao Z et al (2019) Measuring global ocean heat content to estimate the earth energy imbalance. Frontiers in Marine Science 6:432. https://doi.org/10.3389/fmars.2019.00432
Meyssignac B, Ablain M, Geurou A et al (2023) How accurate is accurate enough for measuring sea-level rise and variability. Nat Clim Chang. https://doi.org/10.1038/s41558-023-01735-z
Mimura N (2013) Sea-level rise caused by climate change and its implications for society. Proc Jpn Acad Ser B Phys Sci 89(7):281–301. https://doi.org/10.2183/pjab.89.281
Mittaz J, Bali M, Harris A (2013) The calibration of broad band infrared sensors: time variable biases and other issues. In: Proceedings of EUMETSAT satellite conference, pp 62
Mittaz J, Merchant CJ, Woolliams ER (2019) Applying principles of metrology to historical earth observations from satellites. Metrologia 56(3):032002. https://doi.org/10.1088/1681-7575/ab1705
Mudelsee M (2014) Climate Time Series Analysis: Classical Statistical and Bootstrap Methods, Atmospheric and Oceanographic Sciences Library, vol 51, 2nd edn. Springer, Cham, Heidelberg, New York, Dordrecht, London. https://doi.org/10.1007/978-3-319-04450-7
Mudelsee M (2019) Trend analysis of climate time series: a review of methods. Earth Sci Rev 190:310–322. https://doi.org/10.1016/j.earscirev.2018.12.005
Nerem R (1995) Measuring global mean sea level variations using TOPEX/POSEIDON altimeter data. J Geophys Res Oceans 100(C12):25135–25151. https://doi.org/10.1029/95JC02303
Nicholls RJ, Tol RS (2006) Impacts and responses to sea-level rise: a global analysis of the SRES scenarios over the twenty-first century. Philos Trans R Soc Lond A Math Phys Eng Sci 364(1841):1073–1095. https://doi.org/10.1098/rsta.2006.1754
Patterson HD, Thompson R (1971) Recovery of inter-block information when block sizes are unequal. Biometrika 58(3):545–554. https://doi.org/10.2307/2334389
Piecuch CG, Quinn KJ (2016) El niño, la niña, and the global sea level budget. Ocean Sci 12(6):1165–1177. https://doi.org/10.5194/os-12-1165-2016
Povey A, Grainger R (2015) Known and unknown unknowns: uncertainty estimation in satellite remote sensing. Atmosp Meas Techn 8(11):4699–4718. https://doi.org/10.5194/amt-8-4699-2015
Press WH (1978) Flicker noises in astronomy and elsewhere. Comments Astrophys 7:103–119
Rodell M, Famiglietti JS, Wiese DN et al (2018) Emerging trends in global freshwater availability. Nature 557(7707):651–659. https://doi.org/10.1038/s41586-018-0123-1
Rosenzweig C, Solecki WD, Blake R et al (2011) Developing coastal adaptation to climate change in the New York City infrastructure-shed: process, approach, tools, and strategies. Clim Change 106:93–127. https://doi.org/10.1007/s10584-010-0002-8
Scanlon BR, Zhang Z, Save H et al (2016) Global evaluation of new grace mascon products for hydrologic applications. Water Resour Res 52(12):9412–9429
Scargle JD (1982) Studies in astronomical time series analysis. II-statistical aspects of spectral analysis of unevenly spaced data. Astrophys J 263:835–853. https://doi.org/10.1086/160554
Sen PK (1968) Estimates of the regression coefficient based on Kendall's Tau. J Am Stat Assoc 63:1379–1389
Srinivasan M, Tsontos V (2023) Satellite altimetry for ocean and coastal applications: a review. Remote Sens 15(16):3939. https://doi.org/10.3390/rs15163939
Teunissen P, Amiri-Simkooei A (2008) Least-squares variance component estimation. J Geod 82(2):65–82. https://doi.org/10.1007/s00190-007-0157-x
Teunissen PJ (2018) Distributional theory for the DIA method. J Geod 92(1):59–80. https://doi.org/10.1007/s00190-017-1045-7
Theil H (1950) A rank-invariant method of linear and polynomial regression analysis. Indag Math 12(85):173
Thompson DWJ, Barnes EA, Deser C et al (2015) Quantifying the role of internal climate variability in future climate trends. J Clim 28(16):6443–6456. https://doi.org/10.1175/JCLI-D-14-00830.1

Trenberth KE, Fasullo JT (2012) Tracking Earth's energy: from El Niño to global warming. Surv Geophys 33:413–426. https://doi.org/10.1007/s10712-011-9150-2

Vaníček P (1969) Approximate spectral analysis by least-squares fit. Astrophys Space Sci 4(4):387–391. https://doi.org/10.1007/BF00651344

Watts N, Amann M, Arnell N et al (2018) The 2018 report of the Lancet Countdown on health and climate change: shaping the health of nations for centuries to come. Lancet 392(10163):2479–2514. https://doi.org/10.1016/S0140-6736(18)32594-7

Williams S (2003) The effect of coloured noise on the uncertainties of rates estimated from geodetic time series. J Geod 76:483–494. https://doi.org/10.1007/s00190-002-0283-4

Woolliams, E., Cox, M., Loizeau, X. et al. A Metrological Framework for Addressing Uncertainty in Satellite and In Situ Earth Environmental Observations. Surv Geophys (2025) https://doi.org/10.1007/s10712-025-09916-5

Yang J, Gong P, Fu R et al (2013) The role of satellite remote sensing in climate change studies. Nat Clim Chang 3(10):875–883. https://doi.org/10.1038/nclimate1908

Yip SLP, Ferro CAT, Stephenson DB (2011) A simple, coherent framework for partitioning uncertainty in climate predictions. J Clim 24(17):4634–4643. https://doi.org/10.1175/2011JCLI4085.1

Yoon J, Pozzer A, Chang D et al (2016) Trend estimates of AERONET-observed and model-simulated AOTs between 1993 and 2013. Atmos Environ. https://doi.org/10.1016/j.atmosenv.2015.10.058

Zou CZ, Xu H, Hao X et al (2023) Mid-tropospheric layer temperature record derived from satellite microwave sounder observations with backward merging approach. J Geophys Res 128(6):e2022JD037472. https://doi.org/10.1029/2022JD037472



## Authors and Affiliations

**Kevin Gobron[1,2] · Roland Hohensinn[3,4] · Xavier Loizeau[5] · Claire E. Bulgin[6,7] · Christopher J. Merchant[6,7] · Emma R. Woolliams[5] · Maurice G. Cox[5] · Wouter Dorigo[8] · Thomas Howard[5,9] · Mary Langsdale[10] · Adam C. Povey[11] · Michaël Ablain[12] · Janusz Bogusz[13] · Alexander Gruber[8] · Anna Klos[13] · Jonathan Mittaz[6]**

✉ Kevin Gobron
gobron@ipgp.fr

Roland Hohensinn
roland.hohensinn@issibern.ch

Xavier Loizeau
xavier.loizeau@npl.co.uk

Claire E. Bulgin
c.e.bulgin@reading.ac.uk

Christopher J. Merchant
c.j.merchant@reading.ac.uk

Emma R. Woolliams
emma.woolliams@npl.co.uk

Maurice G. Cox
maurice.cox@npl.co.uk

Wouter Dorigo
wouter.dorigo@geo.tuwien.ac.at

Thomas Howard
thomas.howard@npl.co.uk

Mary Langsdale
mary.langsdale@kcl.ac.uk

Adam C. Povey
adam.povey@le.ac.uk

Michaël Ablain
michael.ablain@magellium.fr

Janusz Bogusz
janusz.bogusz@wat.edu.pl

Alexander Gruber
alexander.gruber@geo.tuwien.ac.at

Anna Klos
anna.klos@wat.edu.pl

Jonathan Mittaz
j.mittaz@reading.ac.uk

[1] Institut de physique du globe de Paris, CNRS, IGN, Université Paris Cité, Paris 75005, France

[2] Géodata Paris, IGN, Univ Gustave Eiffel, Marne-la-Vallée 77455, France

[3] International Space Science Institute, Bern 3012, Switzerland

[4] Scripps Orbit and Permanent Array Center (SOPAC), Institute of Geophysics and Planetary Physics, Scripps Institution of Oceanography, University of California San Diego, La Jolla, CA, USA

[5] National Physical Laboratory (NPL), Teddington, Middlesex TW11 0LW, UK

[6] Department of Meteorology, University of Reading, Reading RG6 6ET, UK

[7] National Centre for Earth Observation, University of Reading, Reading RG6 6ET, UK

[8] Department of Geodesy and Geoinformation, Technische Universitaet Wien (TU Wien), Vienna, Austria

[9] Department of Mathematical Sciences, University of Bath, Bath BA2 7AY, UK

[10] National Centre for Earth Observation, King's College London, London WC2B 4BG, UK

[11] National Centre for Earth Observation, University of Leicester, Leicester LE4 5SP, UK

[12] Magellium, Ramonville-Saint-Agne 31520, France

[13] Faculty of Civil Engineering and Geodesy, Military University of Technology, Warsaw, Poland